Structure and tectonic evolution of the Sierra Blanca Basin

Daniel J. Koning, Geoffrey C. Rawling, Shari Kelley, Fraser Goff, William McIntosh, and Lisa Peters

2014, pp. 209-226. https://doi.org/10.56577/FFC-65.209
Supplemental data: https://nmgs.nmt.edu/repository/index.cfml?rid=2014003

in:

Geology of the Sacramento Mountains Region, Rawling, Geoffrey; McLemore, Virginia T.; Timmons, Stacy; Dunbar, Nelia; [eds.], New Mexico Geological Society 65 th Annual Fall Field Conference Guidebook, 318 p.
https://doi.org/10.56577/FFC-65

This page is intentionally left blank to maintain order of facing pages.

STRUCTURE AND TECTONIC EVOLUTION OF THE SIERRA BLANCA BASIN

DANIEL J. KONING[1], GEOFFREY C. RAWLING[2], SHARI KELLEY[1], FRASER GOFF[3], WILLIAM McINTOSH[1], AND LISA PETERS[1]

[1] New Mexico Bureau of Geology and Mineral Resources, New Mexico Institute of Mining and Technology, Socorro, NM, dkoning@nmbg.nmt.edu

[2] New Mexico Bureau of Geology and Mineral Resources, New Mexico Institute of Mining and Technology, Albuquerque, NM

[3] Department of Earth and Environmental Science, New Mexico Institute of Mining and Technology, Socorro, NM

ABSTRACT—The present structural geometry of the Sierra Blanca Basin is an inward plunging, asymmetric synclinorium, where the eastern limb generally dips more steeply than the western limb. Basin subsidence has preserved 900–1300 m of Cretaceous strata unconformably overlain by 140–800 m of lower to middle Eocene fluvial strata, which in turn are overlain by >1 km of lava flows and volcaniclastic sedimentary rocks related to the Sierra Blanca volcanic field. Northwest- to north-trending anticlines and synclines provide evidence for Laramide contraction on the western margin of the basin. Northeast-trending anticlines and synclines are also found along the eastern side of the basin, generally parallel to the transpressional Pecos buckles. The synclinal structure of the Sierra Blanca Basin has been modified by extensional faulting, characterized by five fault sets: (1) north- to northeast-striking, extensional faults along the eastern margin of the basin and in the interior of the Sierra Blanca massif, many coinciding with and paralleling a major dike swarm between Ruidoso and Capitan; (2) relatively long normal faults, such as the Alamogordo and Godfrey Peak faults, that strike northwest to northeast in the central and southwestern parts of the basin; (3) large-displacement, northwest-striking, oblique-normal faults north of the Three Rivers drainage; (4) low-displacement, west-striking faults south of Oscura that parallel dikes radiating from the center of the Sierra Blanca volcanic field; and (5) northeast-trending faults at the southern margin of the basin.

We interpret a more complex structural history for the basin than past workers, who have restricted basin formation to the Laramide, based largely on past interpretations that Sierra Blanca volcanic strata are not deformed and unconformably overlie lower-middle Eocene strata. We show that lower volcanic strata are indeed deformed and argue that the unconformity at the base of volcanic strata is likely restricted to the southern margin of the basin, where northward tilting created paleotopography. Northwest-oriented extension between 38 and 34 Ma resulted in normal throw for the northeast-striking faults of set 1, down-dropping the eastern part of the basin; related fracturing and jointing facilitated ascension of voluminous magmas associated with Sierra Blanca volcanism. The common observation that dikes locally fill northeast-striking normal faults is consistent with dilation preceding and accompanying igneous activity. Subsidence rates may possibly have waned between 34 and 30 Ma, coincident with a change to more alkalic volcanic composition, based on slower stratal accumulation rates and the presence of unconformities. The north-striking Godfrey Peak fault was active after 28.2 Ma. The northwest-striking Jackass Mountain fault was active around 28.5 Ma, based on a dike of that age that intrudes the fault zone and is brecciated by movement along that fault. By Quaternary time only the Alamogordo fault remained active.

INTRODUCTION

We present an overview of the geologic structures of the Sierra Blanca Basin and discuss its tectonic development. We elucidate a more complex tectonic history than advocated by earlier workers. In particular, we argue that the structure of the Sierra Blanca Basin is a composite of both Laramide contraction and late Eocene to early Oligocene extension.

GEOLOGIC BACKGROUND

The Sierra Blanca Basin is a northeast-trending, elliptical depression situated northwest of Ruidoso (Fig. 1). Previous workers have characterized this depression as a syncline (Wegemann, 1914; Bodine, 1956; Weber, 1964; Kelley and Thompson, 1964). This basin has been described as asymmetrical in cross section view, with a gentler-dipping west limb and a steeper east limb (Kelley and Thompson, 1964). Cross sections drawn from recent geologic mapping are generally consistent with this interpretation, although there are places where the west limb dips more steeply than the east limb (Koning et al., 2014; Rawling, 2012a and 2012b).

Appendix data for this paper can be accessed at:
http://nmgs.nmt.edu/repository/index.cfm?rid=2014003

The basin is readily observable on regional geologic maps by the presence of Cretaceous and Eocene strata surrounded by Triassic and Paleozoic rocks (Fig. 1). The Eocene strata were originally included in the Cub Mountain Formation and contain distinctive, reddish floodplain deposits (Bodine, 1956; Weber, 1964; Lucas et al., 1989). Later, Cather (1991a) proposed to split this unit. Lower, arkosic strata were retained as the Cub Mountain Formation but upper, partly volcaniclastic strata were included in a new unit, the Sanders Canyon Formation. These strata are overlain by a 1–3 km-thick sequence of volcanic flows and volcaniclastic sedimentary rocks of the Sierra Blanca volcanic field (Thompson, 1964, 1966, 1972). The volcanic field largely corresponds with a topographically high region northwest of Ruidoso that we refer to as the Sierra Blanca massif (Fig. 1), whose maximum elevation is 3652 m at Sierra Blanca Peak. Figures 2 and 3 summarize the Cretaceous-Oligocene stratigraphy preserved in the Sierra Blanca Basin.

Structures bound the Sierra Blanca Basin on its west, south, and east sides (Fig. 1, 4). On the west, the west-down, normal-slip Alamogordo fault separates the Sierra Blanca Basin from the younger Oligocene-Quaternary Tularosa Basin. To the south lie the Sacramento Mountains, an east-dipping cuesta formed by a combination of footwall uplift along the Alamogordo fault and erosion (Brown and Phillips, 1999; Peterson and Roy, 2005). At the northern end of the Sacramento Mountains, strata dip

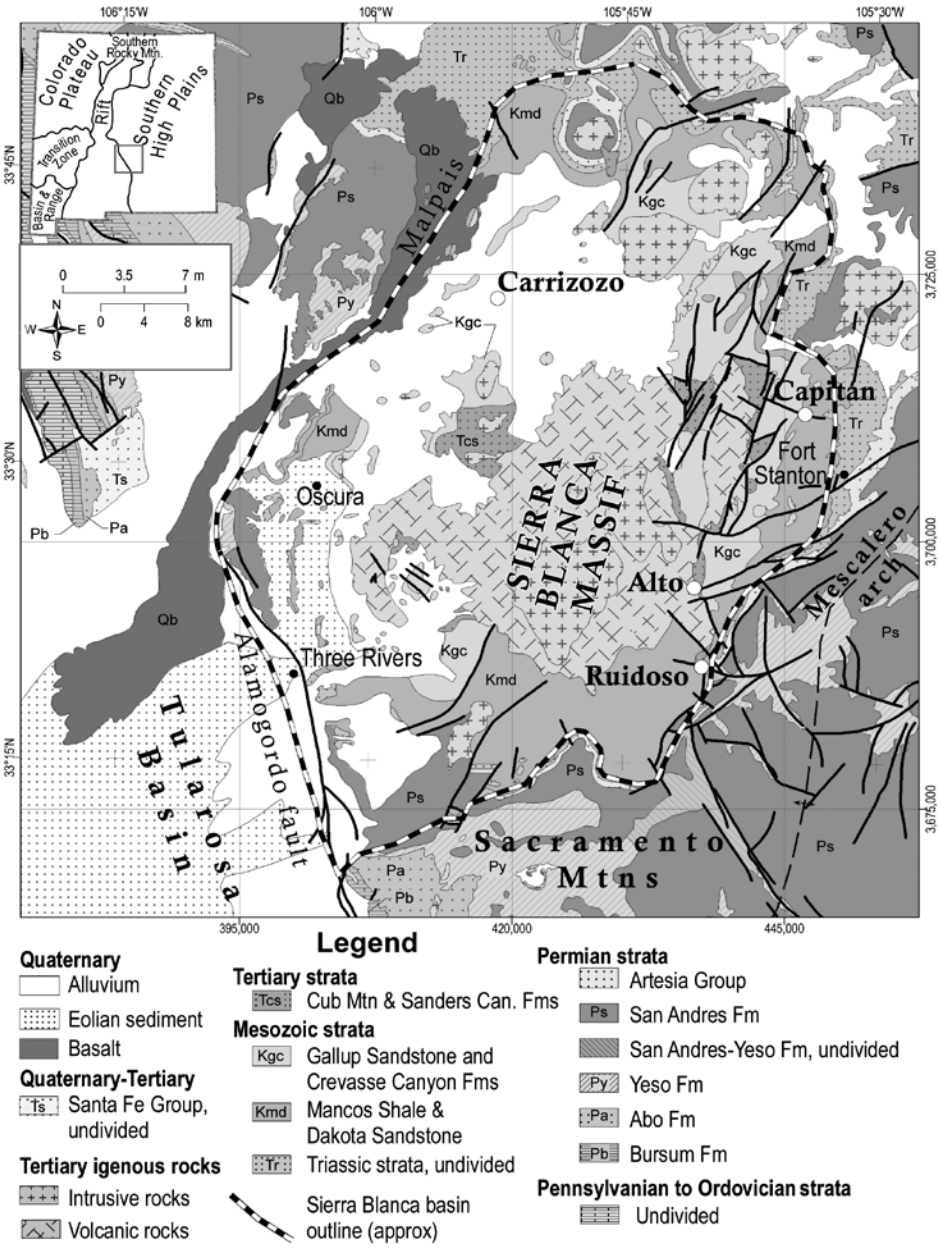

Legend

Quaternary
- Alluvium
- Eolian sediment
- Basalt

Quaternary-Tertiary
- Ts: Santa Fe Group, undivided

Tertiary igenous rocks
- Intrusive rocks
- Volcanic rocks

Tertiary strata
- Tcs: Cub Mtn & Sanders Can. Fms

Mesozoic strata
- Kgc: Gallup Sandstone and Crevasse Canyon Fms
- Kmd: Mancos Shale & Dakota Sandstone
- Tr: Triassic strata, undivided
- Sierra Blanca basin outline (approx)

Permian strata
- Artesia Group
- Ps: San Andres Fm
- San Andres-Yeso Fm, undivided
- Py: Yeso Fm
- Pa: Abo Fm
- Pb: Bursum Fm

Pennsylvanian to Ordovician strata
- Undivided

FIGURE 1. Regional geologic map of the Sierra Blanca Basin. Modified from the state geologic map of New Mexico (New Mexico Bureau of Geology and Mineral Resources, 2003).

northward into the Sierra Blanca Basin across a wide zone of east- to northeast-striking normal faults and flexures (Figs. 1, 4A). Near the east side of the Sierra Blanca Basin is an ~10 km-wide, northeast-striking dike swarm between the towns of Ruidoso and Capitan (Kelley and Thompson, 1964; Elston and Snider, 1964; Cepeda, 1991; Rawling, 2012a, 2012b). The dike swarm also lies on the west limb of the gently northeast-plunging Mescalero arch (Fig. 1). The axis of this arch lies ~10 km east of the dike swarm (Kelley and Thompson, 1964) and is approximately coincidental with the axis of the late Paleozoic Pedernal uplift (Kelley, 1971). No discrete structures define the northeast or northern margins of the basin, and we arbitrarily define the boundary there as coinciding with the base of Cretaceous strata.

Previous ideas regarding basin development

Most previous workers believed the basin formed in the Eocene prior to Sierra Blanca volcanism. Kelley and Thompson (1964) interpreted that basin-related tectonism occurred after deposition of the Cub Mountain-Sanders Canyon succession (which they call the McRae Formation) and prior to Sierra Blanca volcanism, possibly in the late Laramide. This tectonic interpretation was based on a presumed regional unconformity under the base of the Sierra Blanca volcanic field and interpretations that the Sierra Blanca volcanic rocks were relatively horizontal and non-deformed. They also inferred that the Sierra Blanca Basin post-dates the Mescalero arch, since the former appears to deflect the latter (Fig. 1). Kelley and Thompson (1964, p. 118) note that along the southern and southwestern margin of the field, volcanic beds are tilted northward, which they infer to be related to the northerly plunge of post-volcanic uplift of the Sacramento Mountains. Following Weber's (1964) introduction of the Cub Mountain Formation, Kelley (1971) accepted that a regional angular unconformity lay at the base of the Cub Mountain Formation and that this unit overlies older Cretaceous strata to the east. He interpreted this stratigraphic relation as reflecting Laramide tectonic disturbances prior to Cub Mountain deposition. In this modified interpretation, Kelley (1971) allowed for some syn-depositional tectonic activity but maintained that most of the tectonic subsidence of the Sierra Blanca Basin occurred after Cub Mountain deposition and prior to Sierra Blanca volcanism -- a time period he included in the late Laramide. By extension, if the Sierra Blanca Basin is Laramide then the Mescalero arch and the west-down faults between Ruidoso and Capitan are also Laramide features, since subsidence of the basin formed the west limb of this anticline and was apparently accommodated by these faults (Kelley, 1971).

Later workers did not seriously challenge Kelley's tectonic paradigm for the Sierra Blanca Basin. Lucas et al. (1989, p. 16) concur that synclinal down-warping of the basin post-dated deposition of the Cub Mountain Formation, based on paleoflow data that were roughly tangential to the present basin margin rather than being directed towards the basin center. Using petrographic data, Cather (1991a) interpreted that an up-section

increase in basement-derived grains in the Cub Mountain Formation reflected an unroofing sequence of late Laramide uplifts -- implying that the Cub Mountain Formation was deposited during late Laramide tectonism. In his tectonic overview of the Sierra Blanca Basin and Ruidoso region, Cather (1991b, 2002) maintained that the Sierra Blanca Basin is a late Laramide feature but acknowledged uncertainty regarding the kinematic history of many structures. Cather (2002) presented two tectonic scenarios explaining the Sierra Blanca Basin: (1) it is a foreland basin (e.g., similar to the Denver Basin), where tectonic loading along reverse faults produced an asymmetric basin dipping towards an uplift to the southwest (Chapin and Cather, 1981); or (2) it is a product of dextral slip acting along the arcuate trend of the Mescalero arch, causing extensional subsidence in a releasing bend geometry similar to that interpreted for the Eocene-age Galisteo basin to the northwest (Cather, 1992; Abbott et al., 1995).

In this paper, we first summarize the stratigraphy and structure of the Sierra Blanca Basin. Then we demonstrate that Kelley's interpretations supporting a strictly pre-volcanic tectonic origin of the basin are incorrect. Specifically, there is not a regional unconformity at the base of Sierra Blanca volcanic rocks and the volcanic rocks are indeed deformed. Instead, we argue for a two-stage history of basin formation.

METHODS

The data presented in this paper come primarily from geologic mapping conducted in the Sierra Blanca Basin over the past decade (Cikoski et al., 2011; Goff et al., 2011; Kelley et al., 2011; Rawling, 2012a and 2012b; Kelley et al., 2014; Koning et al., 2014). Coupled with this mapping effort, 46 new radiometric ages ($^{40}Ar/^{39}Ar$) were obtained from the New Mexico Geochronology Research Laboratory at the New Mexico Institute of Mining and Technology (Appendix 1; background on laboratory in Heizler and Dunbar, 2014). We use these ages to calculate stratal accumulation rates and the age of cross-cutting intrusions. These ages are presented in Goff et al. (this volume), Kelley et al. (this volume), and Table 1 and Appendix 1 in this paper.

STRATIGRAPHY AND AGE CONTROL

In order to discuss Sierra Blanca tectonism, a summary of the basin's stratigraphy and age control is needed (Figs. 2, 3). The arkosic Cub Mountain Formation contains mammalian fossils interpreted to be ~53–45 Ma (Lucas et al., 1989; Paleobiology Database, 2013), but the overlying, volcaniclastic Sanders Canyon Formation remains undated. The Sierra Blanca volcanic

TABLE 1. Summary of radiometric ages in the Sierra Blanca Basin.

Sample #	Location	Rock Type	Stratigraphic Significance	Easting[1]	Northing	Age (Ma)	Error (±2σ Ma)	Dated mineral or phase	Date quality
10NP6	Sanders Can	syenite	E-W dike	422151	3706009	33.14	0.38	biotite	fair
Tu-1316	8.2 km SSW of Oscura	porphyritic biotite trachyte	E-W-striking dike	399444	3697376	33.35	0.46	biotite	poor*
C-106	Cub Mtn	porphyritic syenite	stock	417323	3710687	34.08	0.21	K-feldspar	**
C-342	Baxter Mountain	porphyritic hornblende trachyte	stock	429830	3734365	34.75	0.18	hornblende	good
08GD-28	Hamm well area	trachybasalt	NE-striking dike	412704	3687347	34.38	0.76	groundmass	poor*
Tu-1470	5 km SE of Oscura	megacrystic dike	NW-striking dike	404830	3700801	34.9	1.4	groundmass	very poor*
08CAT	No. side of Cat Mountain	alkali diorite	thick sill	416020	3672437	36.21	0.30	biotite	fair
09GD07	Crawford windmill area	alkali diorite	NW-stiking dike	411503	3684169	36.41	0.41	groundmass	good
09GD08	Crawford windmill area	porphyritic diorite	N-striking dike that cross-cuts 09GD07	411503	3684169	36.90	0.51	groundmass	poor*
Kitty Spring[2]	Kitty Spring	alkali diorite	thick sill	405032	3680799	37.17	0.33	hornblende	good
08GD-40B	N of Boone Draw	megacystic trachyte	sill	410998	3687059	37.95	0.91	groundmass	good
CM4	Granite well, Temporal Creek	alkali diorite - alkali gabbro	thick sill	407781	3673869	38.07	0.64	biotite	fair

See Appendix 1 for more details on the analytical methods and analyses.

* Disturbed age spectrum, probably affected by recoil

** Age spectrum is precise but other analyses of this sample yielded complicated results. It was first ran as single crystal fusion but analyses revealed a large range of ages. Large single grains were then step-heated. One analysis revealed a disturbed spectrum with ages ranging from 43.04 Ma to 81.68 Ma. The other revealed a well behaved age spectrum, with a weighted mean age calculated from steps C-E of 34.08±0.21 Ma.

1. UTM locations NAD27, zone 13.
2. Erroneously called Kitting Spring in Appendix 1.

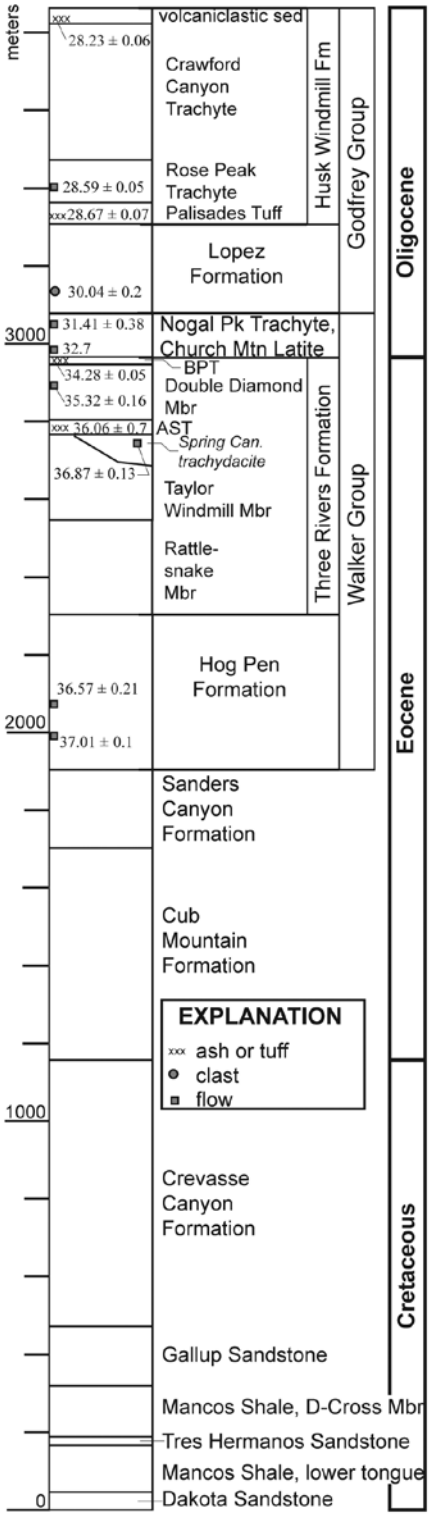

FIGURE 2. Generalized Cretaceous and Eocene-Oligocene stratigraphy of the Sierra Blanca Basin. Note that the thicknesses of volcanic strata (i.e., Walker and Godfrey Groups) are variable and that the Kountz Canyon and Gaylord flows roughly occupy the same stratigraphic position as the Nogal Peak Trachyte and Church Mountain Phonolite. Age control (in Ma) and the material dated is also depicted (see Kelley et al., this volume). AST = Argentina Spring Tuff; BPT = Buck Pasture Tuff; TUNC = tuff of upper Nogal Canyon.

sequence totals 1000–3000 m in thickness and includes two groups: the Walker Group, comprising the Sierra Blanca massif, and the younger Godfrey Group underlying the Godfrey Hills. Kelley et al. (this volume) have differentiated new units of the Walker Group on the western slopes of Sierra Blanca and present their age control (Figs. 2, 3). Summarizing that work, the Hog Pen Formation (37.1–36.7 Ma) is overlain by the Three Rivers Formation (36.7–34 Ma). Both consist of interbedded volcanic flows (relatively alkalic basalt, andesite, and dacite), volcaniclastic sedimentary rocks, and minor tuffs. The Three Rivers Formation contains four members, from oldest to youngest: the Rattlesnake Member, Taylor Windmill Member, Argentina Spring Tuff, and the Double Diamond Member (Figs. 2, 3). In the upper part of the Rattlesnake Member are megacrystic plagioclase-phyric flows informally known as the "turkey-track lavas;" these distinctive lavas are also found higher in the section to the east of the western escarpment (Goff et al., 2011).

Volcanic strata postdating the Three Rivers Formation are generally more felsic than underlying flows, although they still lack quartz. Unconformably overlying the Three River Formation are potassium feldspar- or biotite-bearing flows that include the Nogal Peak Trachyte (31.41 ±0.38 Ma) and flows that fill major paleovalleys including the Church Mountain Phonolite (32.7 Ma), and the Gaylord and Kountz Canyon flows (Figs. 2, 3). The lower Godfrey Group includes the Lopez Formation, consisting of volcaniclastic sedimentary rocks interbedded with various lava flows, overlain by the Husk Windmill Formation (Fig. 2). A clast age of 30.04 ±0.20 Ma from the lower Lopez Formation gives a maximum age constraint for the unit. From bottom to top, the Husk Windmill Formation consists of a discontinuously exposed trachydacite flow, a trachytic tuff (Palisades Tuff, 28.67 ±0.07 Ma), and two flow-dominated units called the Rose Peak Trachyte (28.59 ±0.05 Ma) and the Crawford Canyon Trachyte (Fig. 2). The flows are overlain by 35–45 m-thick sandy conglomerate derived from erosion of the underlying trachyte flows and deposited by streams flowing to the northeast, based on clast imbrication at a single locality. This conglomerate contains a vitric tuff bed that returned a sanidine $^{40}Ar/^{39}Ar$ age of 28.23 ±0.06 Ma (Kelley et al., this volume).

Intrusions in the Sierra Blanca massif provide important relative and absolute age control. Located 12 km southwest of Sierra Blanca Peak, Black Mountain consists of a composite stock that intruded Cretaceous rocks (Fig. 4A). Thermal alteration effects are sparse along the contact between the two intrusions composing the stock, supporting a nearly coeval age (Moore et al., 1991). $^{40}Ar/^{39}Ar$ analyses returned ages of 37.8, 37.3, and 34.6 Ma for the two intrusions (Allen and Foord, 1991), with the 34.6 Ma age being inconsistent with stratigraphic relations expounded on below.

Thousands of dikes and sills crosscut Eocene and older sedimentary strata, the Walker Group, and, to a lesser extent, the Godfrey Group. The Black Mountain stock and surrounding sedimentary rocks are intruded by a major, northeast-trending dike swarm composed of alkali gabbro and monzogabbro characterized by large phenocrysts and xenocrysts of hornblende (as much as 4 cm long). Dikes commonly intrude into the damage zones of steeply dipping, northeast-striking faults. Dioritic

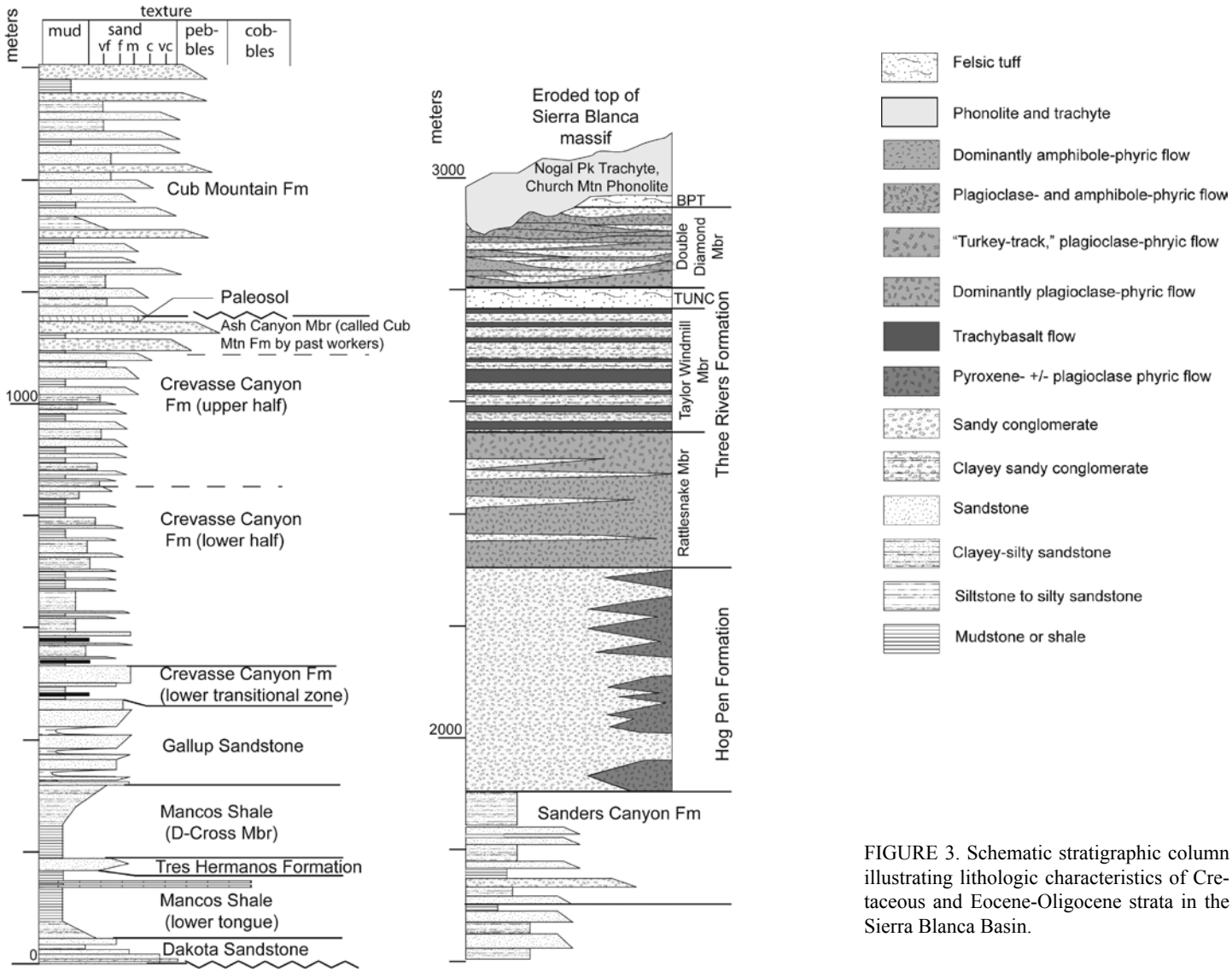

FIGURE 3. Schematic stratigraphic column illustrating lithologic characteristics of Cretaceous and Eocene-Oligocene strata in the Sierra Blanca Basin.

dikes, generally northeast-trending, and sills that may predate the Black Mountain stock are present in the Sacramento Mountains to the south (Pray, 1961) and have returned $^{40}Ar/^{39}Ar$ ages of 44–36 Ma (Asquith, 1974; Miller et al., 1997; Dowe et al., 2002; McLemore, 2002; McManus and McMillan, 2002). The intrusions of Black Mountain, including the northeast-trending dike swarm, are unconformably overlain by volcanic flows and volcaniclastic sedimentary rocks of the Sierra Blanca volcanic field (Fig. 4A).

The most important observations regarding dikes and sills are: (1) sills are mostly composed of megacrystic alkali gabbro or medium-grained diorite between Oscura and the north end of the Sacramento Mountains, but are more diverse north of Oscura where syenite, fine-grained trachyandesite(?), biotite-bearing trachydacite(?), and megacrystic alkali gabbro are present; and (2) south of Oscura, intermediate-mafic sills are generally cross-cut by dikes. West of Sierra Blanca, mafic-intermediate sills in the study area are 38–36 Ma and three mafic-intermediate dikes have poor-quality ages of 37 to ~34 Ma (Table 1). Syenitic intrusions appear to be younger than most mafic-intermediate intrusions, but there is chronologic overlap during 35–34 Ma. The Willow Hill syenite sill is cross-cut by east-west, mafic to intermediate dikes, one of which was K-Ar dated at 34.4 ±1.2 Ma (Weber, 1971), whereas the syenitic Chaves sill and adjoining Cub Mountain stock (34.08 ±0.21 Ma) lack cross-cutting dikes (Table 1, sample C-106). A syenite dike southeast of Chaves Mountain yielded a $^{40}Ar/^{39}Ar$ age of 33.14 ±0.38 Ma from biotite (Table 1, sample 10NP6). Other exposed syenite sills north of Oscura are not cross-cut by intermediate-mafic dikes. From these ages and cross-cutting relations, we infer that dike intrusion activity, particularly mafic-intermediate dikes, waned after 34 Ma.

Most dikes appear to radiate from two igneous centers. The southern center corresponds to a broad area ~15 km in diameter between Sierra Blanca Peak and Nogal Peak. The location of the northern center approximately coincides with Double Diamond Peak. The radiating dike pattern away from this hydrothermally altered area was described by Cikoski et al. (2012).

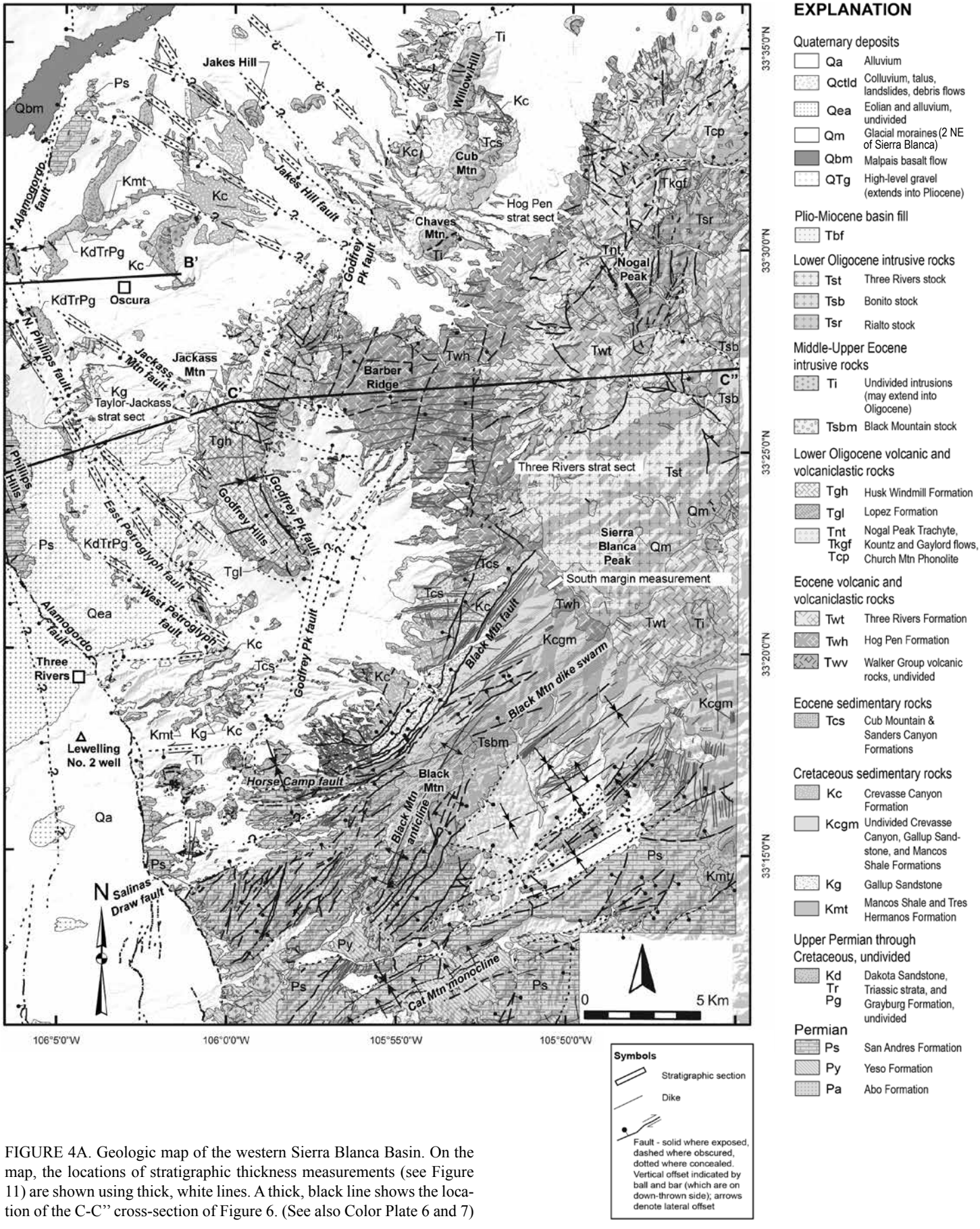

FIGURE 4A. Geologic map of the western Sierra Blanca Basin. On the map, the locations of stratigraphic thickness measurements (see Figure 11) are shown using thick, white lines. A thick, black line shows the location of the C-C'' cross-section of Figure 6. (See also Color Plate 6 and 7)

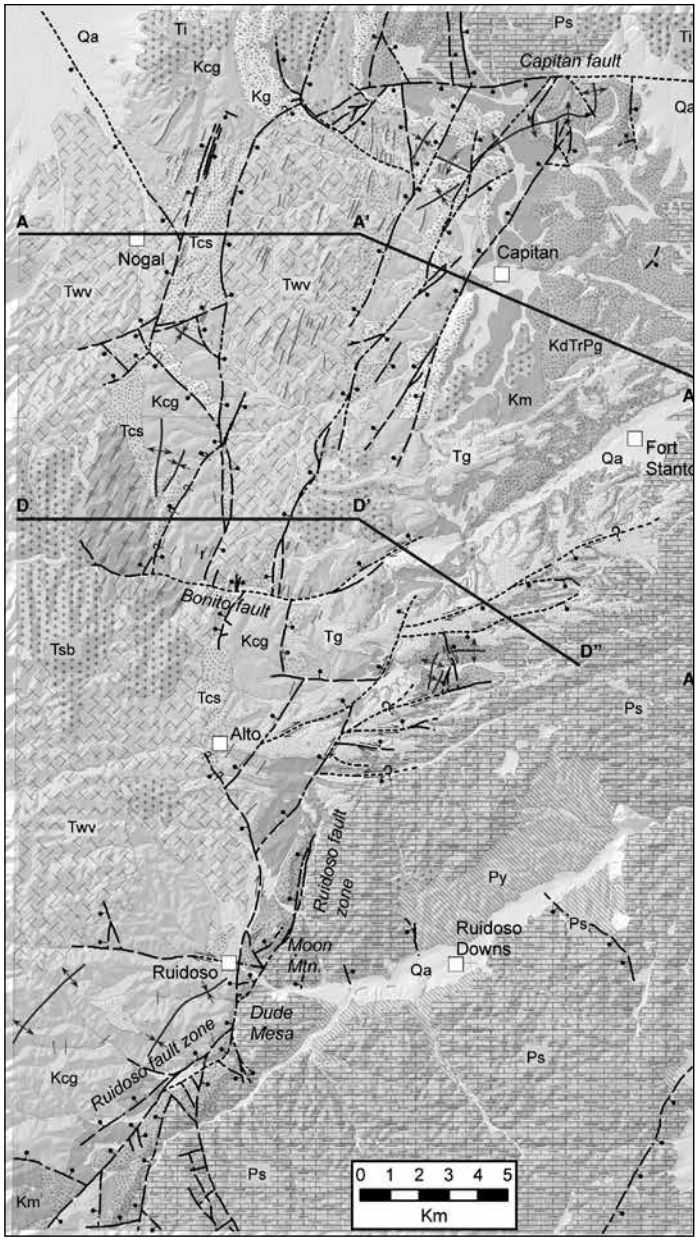

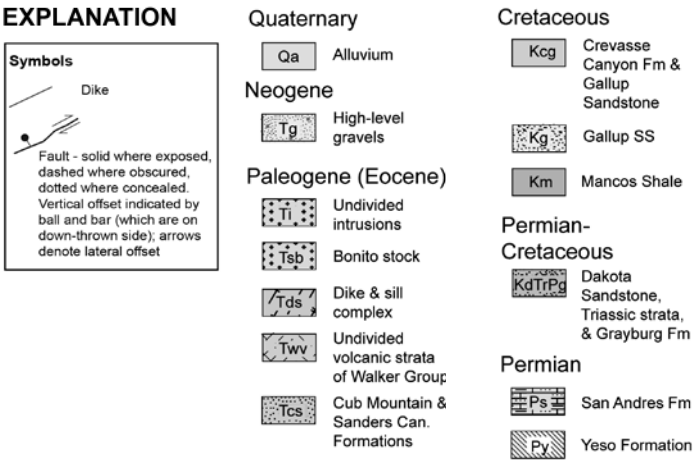

FIGURE 4B. Geologic map of the eastern Sierra Blanca Basin.

STRUCTURE

At present, the structurally deepest portions of the Sierra Blanca Basin coincide with high topography of the Sierra Blanca massif. No major mountain-front faults bound the steep western and northern flanks of the massif, so denudation and differential erosion of a buried volcanic complex likely explains this paradox. Extrapolating from the analyses of Cather et al. (2012), the land surface at the end of Sierra Blanca volcanism would have been above what is now Sierra Blanca Peak by at least 500 m. At least 2 km of erosion occurred in the middle to late Miocene (Cather et al., 2012), removing softer and more erodible strata that lay laterally adjacent to the harder volcanic rocks and creating the present-day escarpments around the massif. Tectonic subsidence of the basin also helped to juxtapose these volcanic rocks against softer Mesozoic strata that were later eroded.

Dip of strata

Volcanic and sedimentary strata dip inwards towards the center of the Sierra Blanca Basin (Figs. 5, 6). On the west side, dips are generally 5–10°E. There is a notable bend in strikes just south of the latitude of Oscura. North of this latitude, the general strike direction is northeast, but to the south of Oscura it is north to northwest. On the north end of the Sierra Blanca massif, strata strike east and dip south. East of Sierra Blanca, between Ruidoso and Nogal-Capitan, strata strike north-northeast and dip 10–30°W. In the interior of the Sierra Blanca massif, bedding orientation is variable but dips are generally less than 9°E except near intrusions and in some paleovalleys (Goff et al., 2011; Cikoski et al., 2011). In places, bedding attitudes vary over such short distances that they average out to be sub-horizontal.

Faults

We differentiate five fault sets in the Sierra Blanca Basin (Figs. 4, 5). The first set corresponds to north- to northeast-striking faults along the eastern margin of the basin and in the interior of the Sierra Blanca massif. Shorter west-northwest faults intersect or branch off of the longer northeast-striking faults. These interconnected faults have been referred to as the Ruidoso fault zone (Kelley and Thompson, 1964). Sense of movement across the faults varies, but motion is dominantly dip-slip and the net effect is west-side down movement of the Sierra Blanca Basin relative to the Mescalero Arch to the east. Maximum vertical displacement is about 600 meters on the Ruidoso fault-zone near Moon Mountain and Dude Mesa in Ruidoso (Fig. 4B). The nearly east-trending network of faults between Alto and Fort Stanton (Fig. 4B) probably has a component of dextral strike-slip motion based on limited slickenside data, map patterns, and well log analyses. The prominent east-west trending, south-down Capitan fault at the south flank of the Capitan Mountains is probably related to the intrusion of the Capitan pluton (Kelley and Thompson, 1964; Rawling, 2012a). North to northeast-striking faults and east-striking faults are also present in the Sierra Blanca massif (Fig. 4A).

North of the Sierra Blanca massif, but included in the first set, is a major northeast-striking fault called the White Oaks fault zone (per Kelley and Thompson, 1964), which extends 23 km from White Oaks to Carrizozo. An exposure 3.3 km southwest of White Oaks indicates synclinal folding immediately adjacent to this fault (Fig. 7). At a location 0.4 km north of this exposure, kinematic indicators and sense of stratigraphic displacement on subsidiary faults to this structure indicate a significant component of strike-slip along the White Oaks fault zone (Koning and Kempter, 2010; Table 2, sites b and c).

The second fault set includes relatively long faults in the central and southwestern part of the basin that strike, on average, northerly (ranging from northwest to northeast, Figs. 4, 5). These faults include the Alamogordo fault and the Godfrey Peak

TABLE 2. Compilation of slickenside measurements on fault planes.

Sample #	Easting*	Northing*	Slip sense	Sub slip sense	Plane dip direction	Plane dip	Slickenslide trend	Slickenslide plunge	Comments
a	413069	3721333	normal dip-slip		347	10	340	10	
b	429103	3731206	dextral strike-slip		289	86	199	0	1
c	429343	3731120	sinistral strike-slip	normal dip slip	335	77	245	8	2
d	422205	3707865	sinistral strike-slip	normal dip-slip	315	47	252	26	
e	398132	3703522	sinistral strike-slip	reverse dip slip	75	85	152	6	
f	397485	3703849	normal dip-slip	sinistral strike slip	55	81	24	80	
g	397025	3705697	normal dip-slip		39	60	35	58	
h	396816	3705934	normal dip-slip	sinistral strike slip	86	73	68	71	
i	396939	3703356	normal dip-slip		235	77	227	77	
j	396437	3693449	normal dip-slip	dextral strike-slip	227	69	235	68	3
k	396622	3703716	normal dip-slip	dextral strike-slip	48	66	92	59	
l	395601	3697046	normal dip-slip		245	75	252	73	4
m	400105	3700998	normal dip-slip	dextral strike-slip	221	36	256	31	
n	399508	3697657	sinistral strike-slip		173	72	87	10	5
o	405150	3693833	dextral strike-slip	normal dip-slip	20	86	105	33	
p	405136	3693802	dextral strike-slip	normal dip-slip	58	83	118	77	
q	419038	3705989	normal dip-slip	sinistral strike-slip	167	85	210	62	
r	405239	3682050	normal dip-slip	sinistral strike-slip	156	73	80	40	
s	404252	3682318	sinistral strike-slip	reverse dip slip	9	90	279	23	
t	404981	3681730	reverse dip-slip	sinistral strike-slip	171	80	229	56	
u	404247	3682918	normal dip-slip	dextral strike-slip	1	66	22	63	6
v	405325	3690755	normal dip-slip	sinistral strike slip	6	65	343	60	
aa	436229	3716583	normal dip-slip	dextral strike-slip	260	55	305	46	7
bb	436057	3714255	normal dip-slip	sinistral strike-slip	135	62	88	52	7
cc	436191	3713212	dextral strike-slip	normal dip-slip	291	87	12	70	7
dd	448267	3717206	sinistral strike-slip	normal dip-slip	145	68	59	11	7
ee	445552	3710337	normal dip-slip	dextral strike-slip	282	79	300	78	7
ff	442428	3706922	sinistral strike-slip	normal dip-slip	127	60	64	39	7
gg	437595	3704350	normal dip-slip	sinistral strike-slip	323	70	312	68	7
hh	442918	3703510	sinistral strike-slip	normal dip-slip	305	70	230	27	7
ii	450285	3704795	sinistral strike-slip	normal dip-slip	305	88	215	5	7
jj	444822	3698366	sinistral strike-slip	normal dip-slip	303	72	252	62	7
kk	440791	3695052	normal dip-slip	sinistral strike-slip	129	69	88	56	7
ll	442228	3694700	dextral strike-slip	normal dip-slip	295	85	25	8	7
mm	436619	3687756	normal dip-slip	sinistral strike-slip	80	74	55	67	7
nn	439745	3686687	normal dip-slip	dextral strike-slip	202	84	230	71	7
oo	436260	3683939	normal dip-slip	sinistral strike-slip	40	85	27	80	7
pp	436619	3701272	normal dip-slip	dextral strike-slip	102	47	115	48	7

Comments:
1. Apparent throw is west-down. Given a SW dip direction of strata, dextral slip is needed.
2. Small conjugate fault; sinistral sense of lateral slip. Maybe a riedal fault to the larger fault 15 m to E.
3. Slip sense based on kinematic indicators and the presence of relatively tall, distinct fault scarps.
4. There's a slight component of right-lateral slip, but fault motion is primarily W-down and normal.
5. Older reverse slip needed to produce the stratigraphic separation. The last rupture event, which produced the near-horizontal slickenlines, was minor compared to previous reverse dip-slip movement.
6. Normal drag folding is also present.
7. Assume normal dip-slip motion; no definitive map or outcrop-scale evidence of shortening or reverse motion has been found.

* UTM locations NAD27, zone 13.

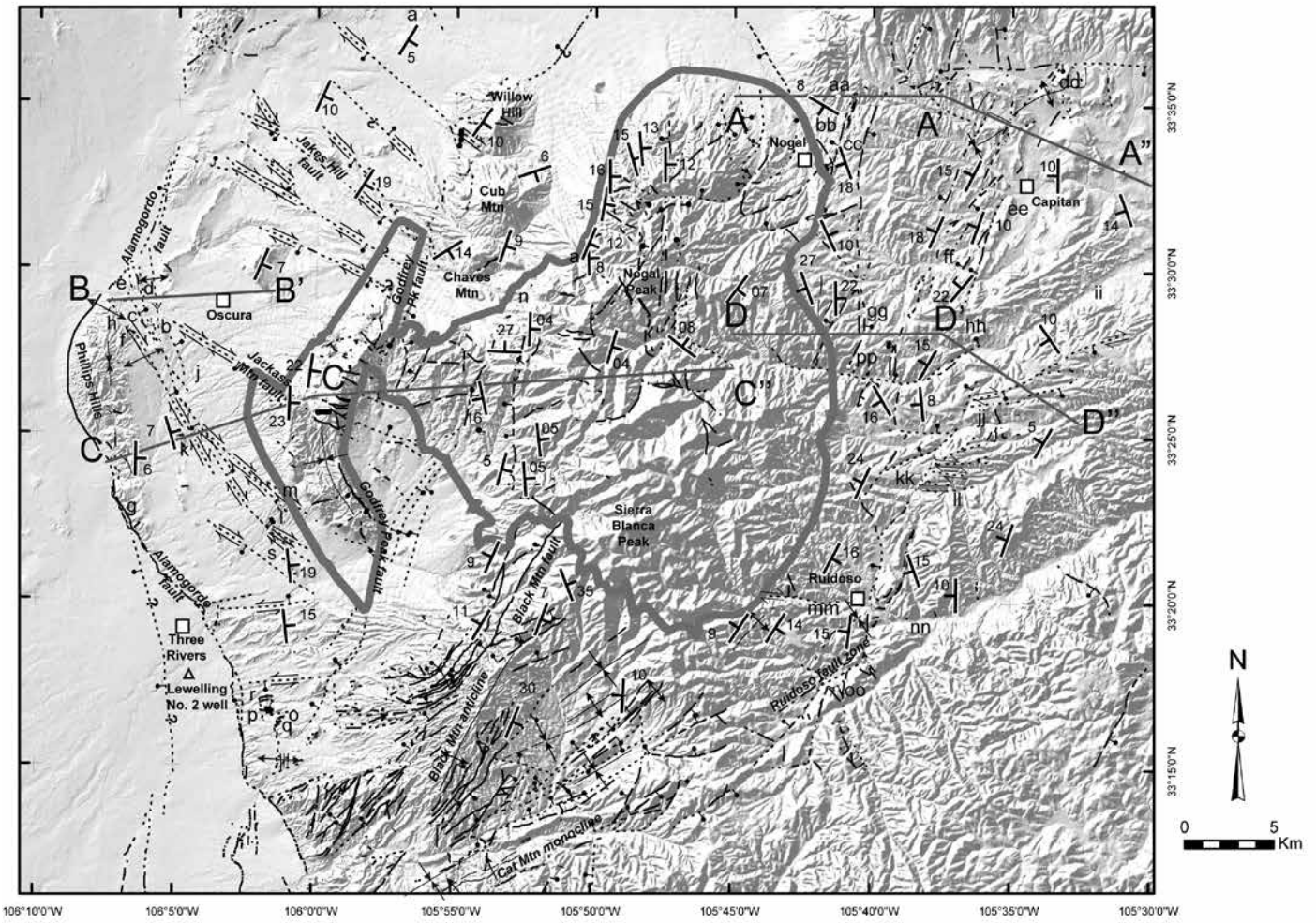

FIGURE 5. Tectonic map of the Sierra Blanca Basin, showing strike and dip of bedding, faults, folds, and locations of cross section lines. The thick, gray line outlines the present margins of the Sierra Blanca volcanic field.

fault. South of Oscura, the Alamogordo fault zone trends northwest, but west of Oscura it bends and strikes northeast (Figs. 4, 5). Eastern strands of the Alamogordo fault zone coincide with scarps probably created by latest Pleistocene movement (Koning et al., 2014). Measurements of slickenside lineations on the eastern fault strand in the southern Phillips Hills indicates almost pure normal, west-down motion (Table 2, site g), although there is evidence it had reverse motion in the Laramide (Koning and Roberts, this volume). The Godfrey Peak fault bounds the eastern side of the Godfrey Hills and continues to ~10.7 km southwest of the southern end of these hills (Fig. 4A).

The third fault set includes large-displacement faults, commonly having several hundred meters of throw, north of the Three Rivers drainage that strike northwest, which we list from southwest to northeast. A northwest-trending fault system extends from the northern end of the Phillips Hills to the Three Rivers Petroglyph site. This fault system includes the North Phillips Hills fault to the north and the western and eastern Petroglyph faults to the south (Fig. 4A). South of Oscura, slickenside lineations at several faulted outcrops, combined with the sense of stratigraphic displacement, indicate both normal and strike-slip fault motion (right-lateral, normal oblique slip) (Table 2, sites l and m). The next fault zone to the northeast is the Jackass Mountain fault, which experienced southwest-down throw and inferred right-lateral slip (Fig. 4A). The Jakes Hill fault passes just south of its namesake (Jakes Hill, 9.5 km north of Oscura).

The fourth fault set includes west-trending faults, which are common south of Oscura and coincide with dike trends. Stratigraphic displacement along these structures generally is less than 30 m, except for the Horse Camp fault (which has ~190 m of north-down throw). Kinematic data southeast of Three Rivers indicate normal oblique slip, with the component of strike-slip being dextral or sinistral (Table 2, sites o-r). At one site 6.4 km southeast of Three Rivers, stratigraphic relations and slickenside measurements indicate almost pure lateral movement superimposed on reverse dip slip.

The fifth fault set includes northeast-trending faults at the south margin of the basin. Included in this set are northeast-striking faults that bound either side of the Black Mountain anticline. The largest of these, the Black Mountain fault, is a northwest-down normal fault (Fig. 4). The Salinas Draw fault is a northeast-striking fault zone with 250–300 m of north-down throw. South of this fault, abundant northeast-striking faults with relatively low throws are present in a 5 km-wide zone (Fig. 4).

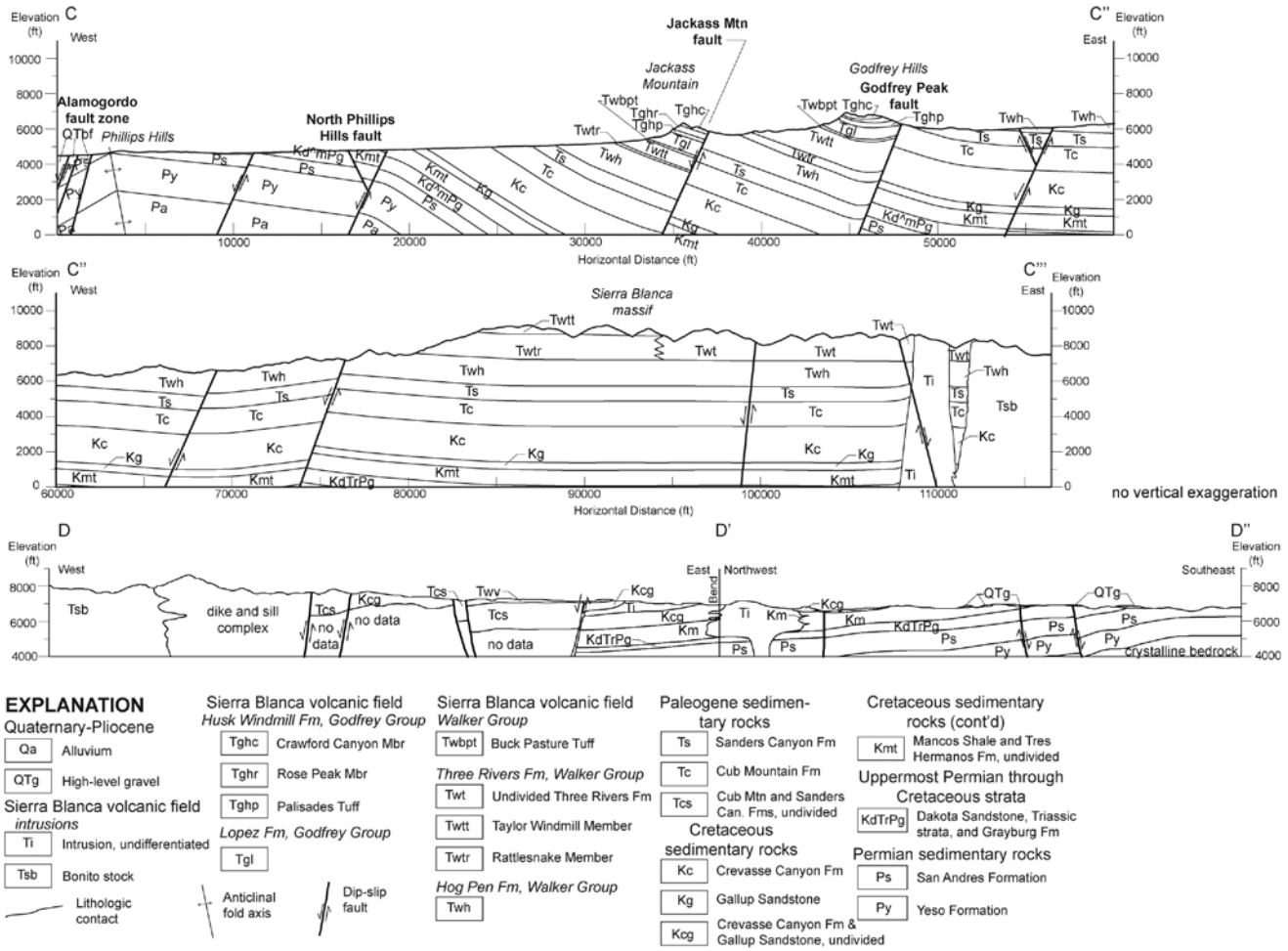

FIGURE 6. East-west cross-sections (C-C'' and D-D'') across the southern, deeper part of the Sierra Blanca Basin. Locations are shown in Figure 5.

Folds

The most prominent fold on the western side of the basin is in the vicinity of cross-section C-C'', between the Alamogordo fault zone and the Godfrey Hills (Fig. 6). Other major folds are found in the northern Phillips Hills and to the north-northeast of these hills (Fig. 5). Here, a south-plunging anticline lies 4 km west of Oscura; this fold has an amplitude of about 200 m and its axis trends slightly west of north (Figs. 4A, 5). A northeast-plunging anticline with an axis trend of 30–40° is exposed at the north end of the Phillips Hills, west of Oscura. Cross-section B-B (Figs. 4A, 5, 8), drawn 0.5 km north of the Phillips Hills, highlights relatively small synclines and anticlines in that area.

Minor folds southeast of Three Rivers have north and northeast trends. At a location 9.5 km southeast of Three Rivers are closely spaced, north-trending anticlines and synclines (Figs. 4A, 5). The aforementioned Black Mountain stock has caused doming of strata (Moore et al., 1991), resulting in the northeast-striking Black Mountain anticline (Figs. 4A, 5; Moore et al., 1988).

Most folds in the eastern half of the Sierra Blanca Basin are subparallel to fault trends (Fig. 4B). Two north-northeast anticline-syncline pairs have been mapped, the first southwest of Ruidoso in the Crevasse Canyon Formation and Gallup Sandstone, and the second south of Nogal (Fig. 4B). The latter appears to fold the Cub Mountain Formation as well as Cretaceous rocks. Northeast-trending, fault-parallel folds are also present north of Capitan.

Folds on the southern margin of the Sierra Blanca Basin strike northeast, parallel to fault and dike trends. A northeast-striking monocline dips 30–65°NNW and affects the Yeso Formation on the north side of Cat Mountain (Fig. 5). Parallel to this monocline to the northwest is a northeast-plunging, faulted syncline. The structural relief of this monocline-syncline pair is 270 m. Domal features, locally associated with thick sills and syenite intrusions, are present between the syncline and the Salinas Draw fault.

We interpret several northeast-trending folds and faults southeast of Black Mountain, based on dip relations shown in Moore et al. (1988). However, these workers explain the structural relief by a fault and graben structure. Based on the trend of transpressional folds to the northeast and east (e.g., the Pecos buckles), we think the folds southeast of Black Mountain are likely related to contraction but we cannot rule out the possibility that the dip patterns are related to drag or tilting along the numerous northeast-striking faults in the area.

DISCUSSION

Validity of two observations supporting the Kelley model

Vincent Kelley used two observations in his interpretation that subsidence of the Sierra Blanca Basin occurred prior to emplacement of the Sierra Blanca volcanic field and after much of the Cub Mountain and Sanders Canyon Formations were deposited: (1) the presence of a regional unconformity beneath the volcanic field, and (2) the volcanic units are relatively undeformed (Kelley and Thompson, 1964; Kelley, 1971). We argue that both of these observations are incorrect.

In regards to the first observation, we interpret that a basal unconformity exists only on the south end of the volcanic field, in the area mapped by Moore et al. (1988). North of here, bedding dips are concordant on either side of the basal contact and the Sanders Canyon Formation grades up into, and locally intertongues with, the Hog Pen Formation (consistent with interpretations by Cather, 1991a). Indeed, rapid emplacement of Hog Pen debris flows and lavas onto saturated, weakly consolidated Sanders Canyon sediment locally resulted in loading and formed a wavy contact geometry, with tens of meters of relief near Barber Ridge (Kelley et al., 2011). This loading also caused injection of clastic dikes of Sanders Canyon sediment into the lower Hog Pen Formation (Koning et al., 2014). Therefore, deposition seems to have been relatively continuous in the center of the basin during the middle to late Eocene.

In regards to the second observation, new geologic mapping indicates that volcanic strata are actually deformed, particularly the Hog Pen Formation and the lower Three Rivers Formation (Koning et al., 2014). Northwest and southwest of Nogal Peak, for example, lower Walker Group strata (i.e., the Hog Pen Formation) commonly dip 4–16° (Fig. 5), although variable dips at Barber Ridge (Kelley et al., 2011) may be ascribed to constructional topography associated with volcanic edifices. Stratigraphically higher volcanic strata dip less, generally 4–8°, as exemplified south of Nogal Peak (Fig. 5); this up-section decrease in dip strongly suggests emplacement of the Walker Group during tectonic tilting.

FIGURE 7. Photograph of the White Oaks fault zone, at an exposure 3.3–3.4 km southeast of the town of White Oaks. View is to the north. White lines follow bedding contacts. The main fault strand, indicated by the white arrows, strikes 050° and dips 82° E. Stratigraphic offset, based on map relations, is east-side-down and so this is not a drag fold. The folding may be related to transpression in the Laramide.

Synthesis of basin development

Although previous workers viewed the Sierra Blanca Basin as a Laramide-age feature, we argue that post-Laramide, extensional tectonism between 38 and 25 Ma made a significant contribution to the current structural configuration of the basin. In the following, we discuss this two-stage structural history of the Sierra Blanca Basin.

Stage 1: Laramide tectonism (early to middle Eocene)

In the Laramide, the Sierra Blanca Basin may have been a Denver-type basin tilted to the west towards a reverse-fault bounded, Laramide uplift in what is now the northern Tularosa Basin (Fig. 9; Chapin and Cather, 1981; Koning and Roberts, this volume). This hypothesis is currently the topic of graduate research by Logan Roberts (NM Tech). Preliminary data supporting this interpretation thus far include: (1) thickening of the Cub Mountain-Sanders Canyon Formations and concomitant strata to the southwest, based on map measurements (Koning and Roberts, this volume, fig. 12); (2) thickening of underlying Crevasse Canyon strata to the southwest in the central and eastern Sierra Blanca Basin (Koning and Roberts, this volume); and an unconformity at the base of the Cub Mountain Formation that displays a slight angular discordance (Kelley, 1971). The Crevasse Canyon Formation (Upper Cretaceous) is only 300 m thick in an oil well on the west side of the Alamogordo fault compared to 670–700 m (2200–2300 ft) to the east of the fault (based on map measurements using Koning et al., 2014), suggesting that the fault experienced west-side-up movement and footwall erosion in the Laramide, which culminated in southern New Mexico during the Paleocene and early to middle Eocene (Seager, 2004). However, this thickness contrast might also be explained by a cryptic normal fault within the Crevasse Canyon Formation at the well.

Fold axes within 5 km east of the Alamogordo fault are consistent with shortening across the fault during regional Laramide contraction (Fig. 9). The north to northwest orientations of fold axes suggests east to northeast vergence, consistent with that interpreted by Seager (2004) for the Las Cruces area. We note, however, the possibility of folding induced by gravity-driven deformation of the underlying, gypsum-rich Yeso Formation, which we suspect may account for west-trending folds in the Phillips Hills (Fig. 5). The contractional features observed on the southern White Oaks fault (Fig. 7) may be associated with

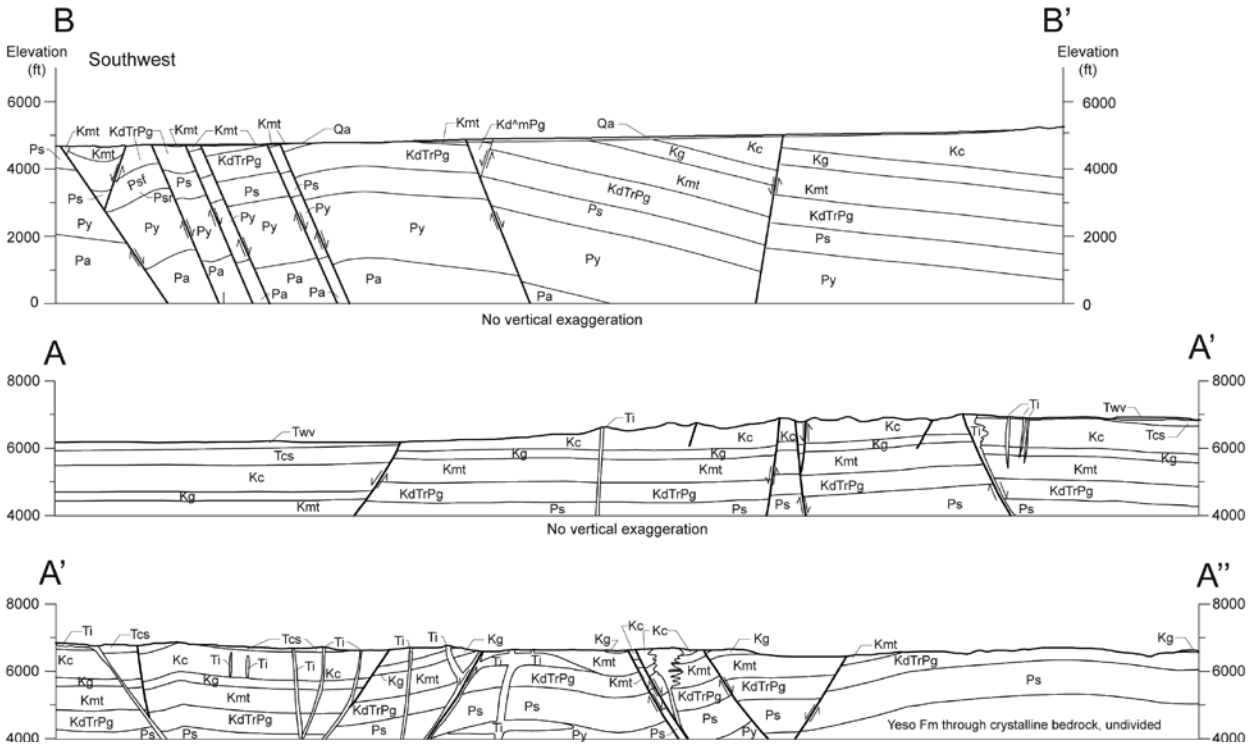

FIGURE 8. East-west cross sections, A-A'' and B-B', illustrating folds on the west and east side of the Sierra Blanca Basin. Their locations are shown on the tectonic map of Figure 5.

east-northeast compression in the Laramide or possibly transpression along a geometrically irregular fault plane.

Several folds are present in the eastern Sierra Blanca Basin near Ruidoso (Fig. 4B), but the general structure is a monoclinal down-warping, broken by faults, towards the center of the Sierra Blanca Basin to the west (Fig. 6). One of the larger folds is a northeast-trending anticline mapped 6 km west of Ruidoso (Figs. 4B, 5). There are also northeast-striking folds north of Capitan and south of Nogal (Figs. 4B, 8). Rather than developing long, north- to northwest-striking folds, the crust near Ruidoso appears to have reacted to Laramide compression in part by strike-slip movement along northeast-trending faults accompanied by transpressional folding (Figs. 4B, 5, 9). These faults parallel the trend of the Pecos buckles to the southeast (Kelley, 1971) and appear to be structurally related to these buckles. The amount of dextral slip is small, however, being on the order of hundreds of meters.

Another hypothesis explaining basin subsidence in the Laramide involves a releasing bend in Laramide structures coinciding with the northwest- to north-striking Alamogordo fault and the Ruidoso fault zone (Fig. 9, panel B). In this scenario, the Alamogordo and Ruidoso faults would undergo right-lateral transpression in response to northeast-southwest compression, and the releasing bend structures in the right step-over between them would include the east- to northeast-striking faults between Three Rivers and the Cat Mountain monocline. It is clear that the northeast-striking faults underwent significant throw prior to Sierra Blanca volcanism and many of these faults are in-filled by Sierra Blanca dikes (Moore et al., 1988; Kelley and Kempter, 2008), so they could have been active in the Laramide. Alternatively, the northeast-striking faults between Three Rivers and Cat Mountain could be a result of post-38 Ma northwest-directed extension (see below), and the north limb of the aforementioned syncline north of the Cat Mountain monocline could be a manifestation of a southwestward continuation of anticlinal doming associated with the Black Mountain stock. This hypothesis would be consistent with dextral slip on the more northerly striking faults associated with the Ruidoso fault zone. Because the amount of dextral slip on the Ruidoso fault zone is relatively small (hundreds of meters), the releasing bend hypothesis seems inadequate, on its own, to create the 600–750 m of regional accommodation space for the Cub Mountain-Sanders Canyon Formations. Another problem with this hypothesis is that folds in the Ruidoso-Capitan area trend northeast, parallel to the Pecos buckles to the east, which is inconsistent with a regional northeast-directed shortening needed to produce the releasing bend. Rather, these folds, and the Pecos Buckles to the east-southeast, are more consistent with east-west contraction (Fig. 9). These two hypotheses are not mutually exclusive. For example, a releasing bend could have co-existed with a Denver-type, west-tilted Laramide basin.

Stage 2: Late Eocene-Oligocene Extension

Late Eocene extension: dike evidence

We interpret tectonic extension in the Ruidoso area beginning ca. 38 Ma, accompanied by subsidence northwest of Ruidoso and concomitant with emplacement of the lower Walker Group. The inception of extension here is slightly earlier than

that interpreted in the northeastern Mogollon volcanic field and southern Rio Grande rift (38 Ma v. 36 Ma; Cather, 1990; Mack, 2004). However, this date agrees with preliminary petrologic studies in the Sacramento Mountains, which note that 44–36 Ma dikes and sills compare more favorably with Rio Grande rift basalts than with back arc or subduction-related magmas (McManus and McMillan, 2002). This post-38 Ma extension explains the ubiquitous northeast-trending dikes in the Sacramento Mountains (Pray, 1961; McManus and McMillan, 2002) and along the Ruidoso fault zone (Kelley and Thompson, 1964; Cepeda, 1991; Rawling, 2012a and 2012b); note that the latter do not radiate away from inferred volcanic centers at and north of Sierra Blanca Peak. The dikes along the Ruidoso fault zone and in the Capitan swarm intrude older normal faults and are commonly faulted along their margins (Bodine, 1956; Rawling, 2012a and 2012b). These facts and the huge volume of dikes (the Capitan swarm composes 25–80% of the total rock volume) indicate magma was injected into northeast-trending, dilational fractures and faults during a time of northwest-directed extension. Because anticlines of presumed Laramide age mostly trend northeast in the Capitan-Ruidoso area, we argue that this northwest-directed extension post-dates the Laramide.

The dikes in the Ruidoso-Capitan area are too altered for radiometric dating, but stratigraphic cross-cutting relationships in terrain southwest of Sierra Blanca Peak allow us to constrain dike inception. There, northeast-trending dikes mapped by Moore et al. (1988) clearly cross-cut the 37.8–37.3 Ma Black Mountain stock but generally do not cross-cut overlying volcanic flows of the Walker Group (Figs. 4A, 10). These flows contain the conspicuous megacrystic plagioclase-phyric flows ("turkey-track" flows) that appear to correlate northward to similar lavas in the upper Rattlesnake Member of the Three Rivers Formation, which were

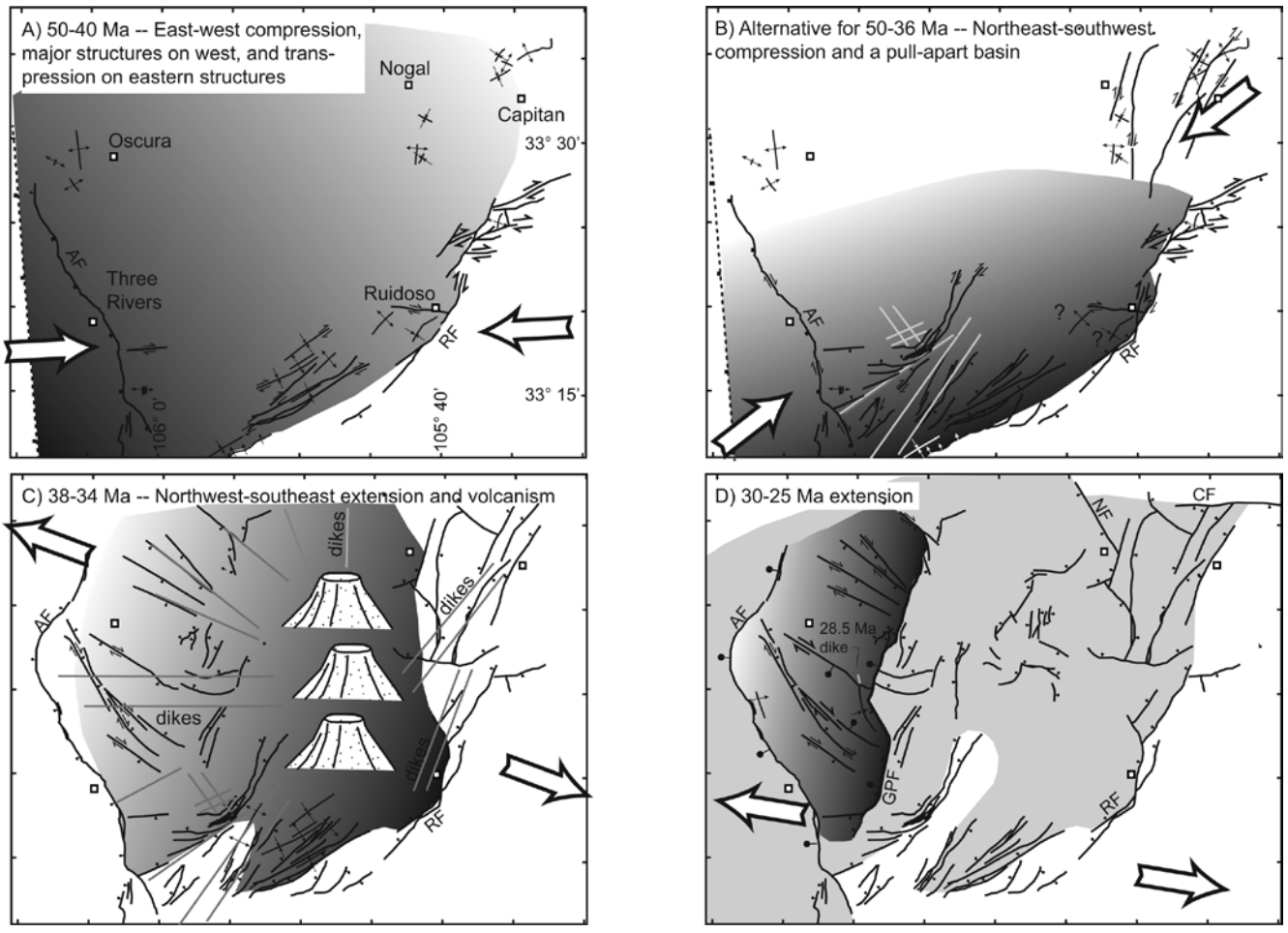

FIGURE 9. Four maps illustrating inferred activity of structures at different time periods. The locations of various towns are labeled in A and denoted by squares. These squares are shown in the rest of the panels for reference. The intensity of the shading conveys relative subsidence rates, with darker shades indicating higher rates. Larger and bolder strike slip arrows or ball-bars alongside faults are drawn where there is relevant kinematic control (generally from slickenside lineations). Otherwise, fault motions are extrapolated from faults with direct kinematic measurements or inferred from stratigraphic and geologic relations. Note that timing of folds in the south-central part of the map is not well-constrained. They could have formed during Laramide compression or possibly during extensional fault block tilting during 38–34 Ma. Panels A and B: two interpretations for the late Laramide. The large, white arrows denote the dominant shortening direction. The queries in panel B are for folds whose geometries seem inconsistent with a northeast shortening direction. Panels C and D: inferences of structural activity for 38–34 Ma and 30–25 Ma, respectively. The length of the 28.5 Ma dike is exaggerated. Abbreviations are: AF = Alamogordo fault; GPF = Godfrey Peak fault; RF = Ruidoso fault zone; NF = Nogal fault; CF = Capitan fault.

erupted about 36.7–36.5 Ma (Fig. 2). If this correlation is correct, this dike swarm was mostly emplaced between 37.3 and 36.7 Ma. Because the phenocrystic content of the intermediate-mafic dikes in the Capitan swarm and the Ruidoso area are broadly similar to Hog Pen and Three Rivers strata, we assume they are roughly the same age (i.e., 37.1–34 Ma). Therefore, northwest-directed extension and dike formation were occurring between 38 and 34 Ma.

Dikes do not parallel the trends of major north-trending faults to the west of the Ruidoso fault zone, such as the Godfrey Peak fault or the Alamogordo fault. The Alamogordo fault is far from the center of Sierra Blanca activity and that may account for this observation. But west and northwest-trending dikes are abundant near the north end of the Godfrey Peak fault. The fact that these dikes do not intrude north- to northeast-trending faults near the north end of the Godfrey Peak fault suggests that the northern fault zone may not have been present during dike emplacement. One brecciated and altered dike was observed filling a fault in the middle portion of the Godfrey Peak fault zone (UTM 408350 m E; 3695885 m N; zone 13, NAD27).

In contrast to the north-trending faults, there is a strong correspondence of mafic-intermediate dike trends with northwest-striking faults between Oscura and Carrizozo (fault set 3). Few of these dikes extend into the Godfrey Group, indicating they are pre-30 Ma in age. This correspondence is suggestive of a genetic linkage between the two, probably related to dilational stresses at dike tips or above their tops (e.g., Rubin, 1992). Some of the faults that experienced several hundreds of meters of displacement, such as the Jakes Hill and Jackass Mountain faults, likely responded to multiple episodes of extension that are concomitant with and post-date the Sierra Blanca volcanic field. We use these dike-fault relations to infer that activity along the northwest-trending fault set (set 3) occurred prior to many faults in the north-trending set (set 2).

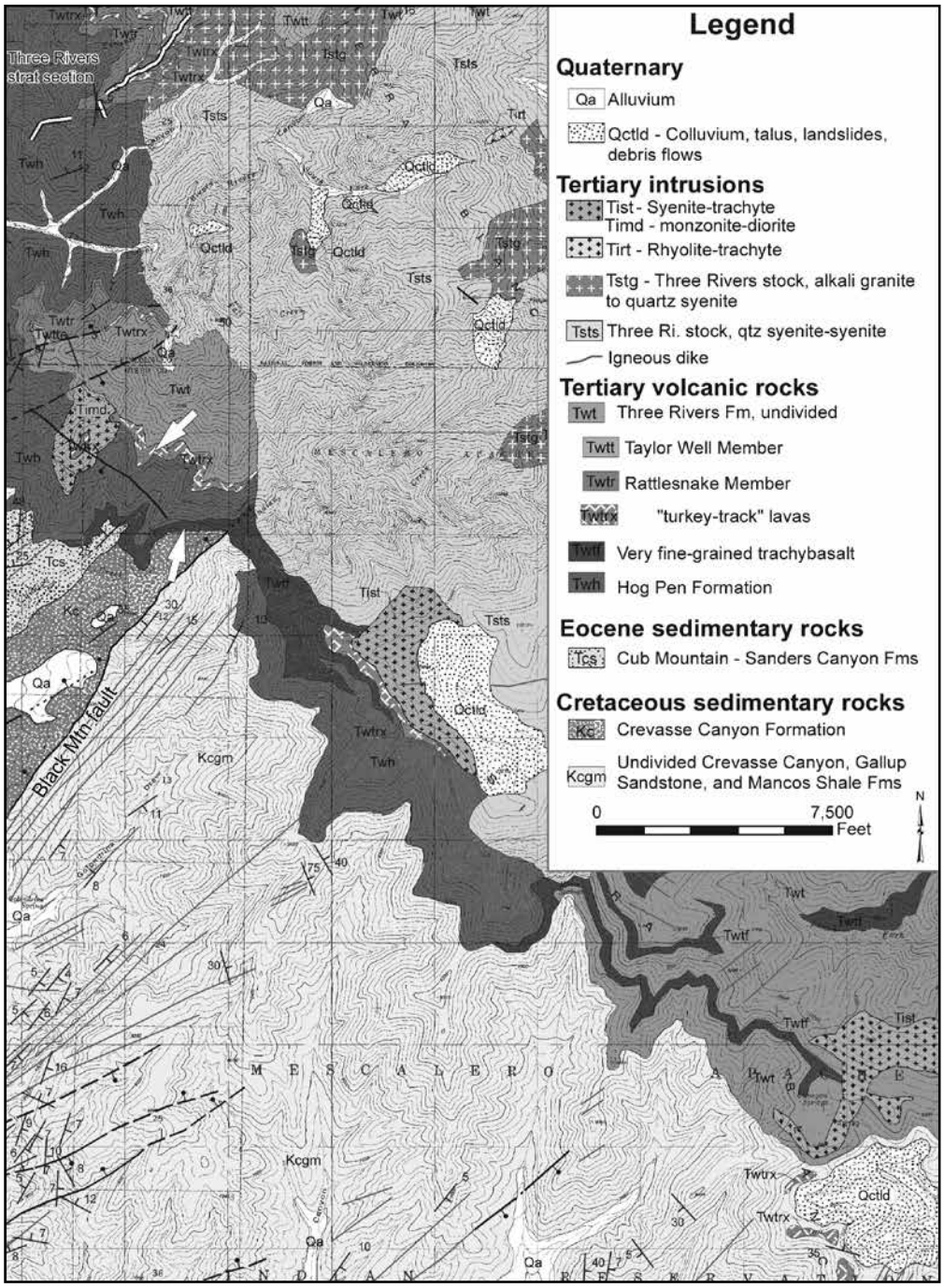

FIGURE 10. Geologic map of the southwestern margin of the Sierra Blanca volcanic field, where it overlies older strata with angular unconformity (from Moore et al., 1988, and Goff et al., 2011). The white arrows denote the relatively flat "turkey-track flows" and the more steeply dipping, fine-grained trachybasalt flows at the base of the Hog Pen Formation. Note how the intervening Hog Pen Formation thickens northward. These relations indicate a component of northwest tilting during emplacement of these strata.

Late Eocene extension: dip and stratigraphic thickness evidence

We interpret that extension between 38 and 34.3 Ma also resulted in west-down throw and flexure along the Ruidoso fault system, which facilitated eastward tilting of the Sierra Blanca Basin (Fig. 9, panel C). This late Eocene, asymmetric subsidence of the Sierra Blanca Basin is supported by the 3–19° eastward dips of strata in the Sierra Blanca volcanic field (Fig 5). The subsidence and tilting

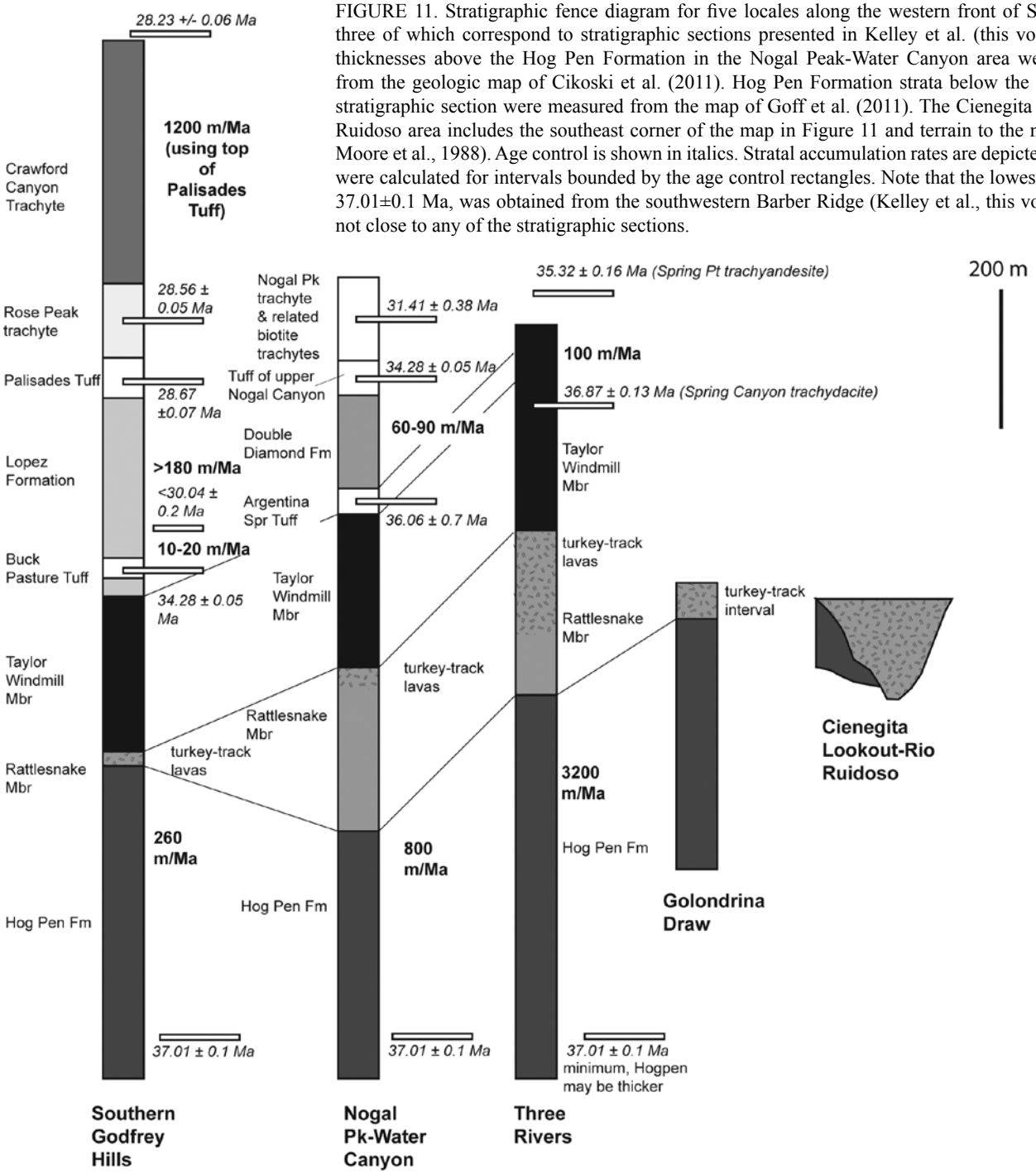

FIGURE 11. Stratigraphic fence diagram for five locales along the western front of Sierra Blanca, three of which correspond to stratigraphic sections presented in Kelley et al. (this volume). Strata thicknesses above the Hog Pen Formation in the Nogal Peak-Water Canyon area were measured from the geologic map of Cikoski et al. (2011). Hog Pen Formation strata below the Three Rivers stratigraphic section were measured from the map of Goff et al. (2011). The Cienegita Lookout-Rio Ruidoso area includes the southeast corner of the map in Figure 11 and terrain to the northeast (see Moore et al., 1988). Age control is shown in italics. Stratal accumulation rates are depicted in bold and were calculated for intervals bounded by the age control rectangles. Note that the lowest age control, 37.01±0.1 Ma, was obtained from the southwestern Barber Ridge (Kelley et al., this volume) and is not close to any of the stratigraphic sections.

was likely accommodated by west-down movement and flexure along the Ruidoso fault system, consistent with the hundreds of meters of west-down throw on these faults. The asymmetric subsidence is also consistent with thickness trends of Sierra Blanca volcanic strata (Fig. 11), where Hog Pen and lower Three River Formation strata are thickest towards the southeast (i.e., at the Three Rivers stratigraphic section). However, we recognize that using thickness trends to infer subsidence in volcanic strata is significantly complicated by local thickening associated with specific eruptive centers. We depict stratal accumulation rates on Figure 11 for Sierra Blanca volcanic and volcaniclastic strata and note a significant reduction of rates between 36–34 Ma and 30 Ma. This decrease may reflect a decrease in lava extrusion rates that perhaps was accompanied by a waning of tectonic subsidence.

Other evidence for tectonic subsidence during the late Eocene comes from geologic map relations on the southern margin of the basin (Fig. 10), where local, steep contacts suggest buttress stratigraphic relations and filling of paleotopography (Moore et al., 1988). Near the northeast end of the Black Mountain fault, Moore et al. (1988) show fine-grained trachybasalt flows (unit Twtf on Fig. 10) dipping to the north parallel with the basal

Hog Pen contact but the "turkey-track" lavas (unit Twtrx) are much flatter, based on their map pattern (Fig. 10). This discordance in dips indicates tectonic tilting occurred between emplacement of the lower trachybasalt flows and the "turkey-track flows," which is consistent with the north-thickening wedge of Hog Pen lavas between these flow packages. The Black Mountain fault does not significantly offset lower Walker Group strata, although fault movement along a possible buried, northeast extension of this fault may have produced a northwest-down, monoclinal drape fold in these strata (Fig. 10; Moore et al., 1988). This suggests that the normal fault experienced most of its activity prior to 37 Ma (the age of the lower Hog Pen Formation, Fig. 2), perhaps in a releasing bend in the Laramide or during northwest-directed extension during 38–37 Ma.

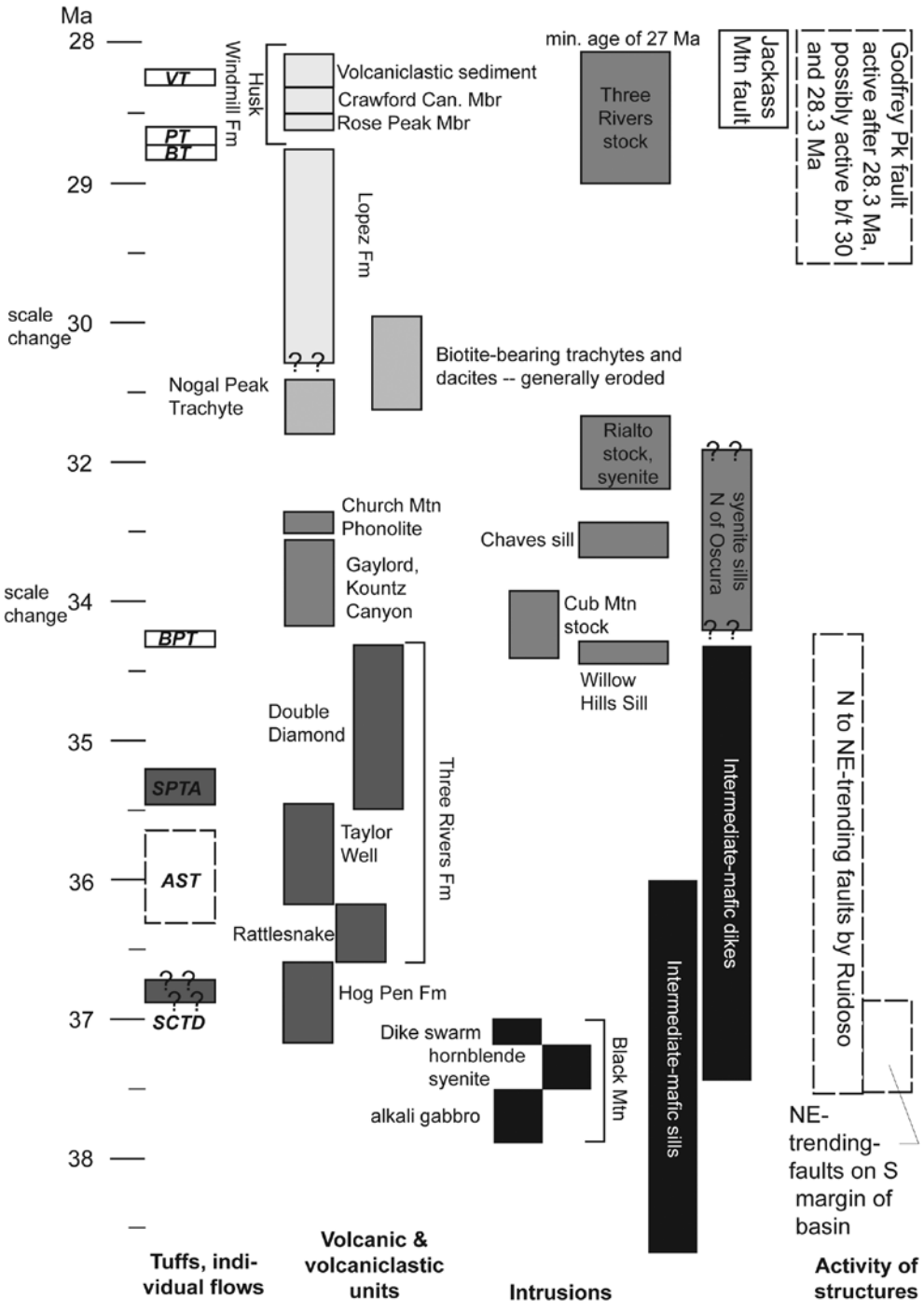

FIGURE 12. Interpreted timing of extensional tectonism and major phases of igneous activity in the Sierra Blanca Basin. Abbreviations for the tuff (left column) are: SCTD = Spring Canyon trachydacite; AST = Argentina Spring Tuff; SPTA = Spring Point trachyandesite; BPT = Buck Pasture Tuff; BT = biotite trachyte; PT = Palisades Tuff; and VT = vitric tuff.

Oligocene tectonic activity

Compared to the predominance of mafic-intermediate composition lavas at 37.1–34 Ma, a higher degree of alkalic intrusions and volcanism occurred between 34 and 30 Ma. This alkalic volcanism filled major paleovalleys cut into pre-34 Ma volcanic strata on the north end of the Sierra Blanca massif, near Church Mountain (e.g., units Tcp and Tkgf in Fig. 4A; Cikoski et al., 2011). These paleovalleys presumably drained northward, away from the center of the Sierra Blanca volcanic field. If tectonic subsidence at this time was greatest over the deepest part of the basin (i.e., near the center of the volcanic field), then the headwaters of the paleovalleys would be at the area of greatest subsidence. Therefore, erosion of these paleovalleys suggests that subsidence slowed between 34 and 30 Ma, allowing streams to cut deeper canyons than before. Another possibility is increased magma output and rates of topographic build-up in the center of the volcanic field during 34–30 Ma, compared to the northern Sierra Blanca field, which would have increased drainage gradients and discharge and resulted in increased stream power.

After a period of low stratal accumulation rates, unconformities (e.g., the lava-filled paleovalleys), and alkalic intrusions and volcanism between 34 and 30 Ma (Figs. 11, 12), there is evidence for tectonic activity on the Jackass Mountain and Godfrey Peak faults in the Early Oligocene. A 28.53 ±0.03 Ma dike intrudes the Jackass Mountain fault and is brecciated by subsequent movement along that fault. The dike fills a northwest-striking fracture

as well, consistent with a right-lateral strike-slip component of motion during west-directed extension (Fig. 9, panel D).

The earliest evidence of possible activity on the Godfrey Peak fault is 28.2 Ma, when there may have been syntectonic deposition of the upper volcaniclastic unit of the Husk Windmill Formation in a syncline in the southern Godfrey Hills (Figs. 4, 5). This syncline is interpreted to be related to a fault-propagation fold or perhaps drag-folding in the hanging wall of the Godfrey Peak fault and a northwest-striking fault northeast of the East Petroglyph fault. Evidence for syntectonic deposition includes: (1) northeastward paleoflow indicators in the upper volcaniclastic unit of the Husk Windmill Formation that are directed towards the fault (Kelley et al., 2011); (2) a possible, low-angle buttress unconformity at the north end of the volcaniclastic sediment, where it overlies the Crawford Canyon Member of the Husk Windmill Formation; and (3) clasts from Crawford Canyon trachyte flows in the volcaniclastic sedimentary rocks, consistent with erosion of volcanic flows along the tilted margins of the syncline. Also, there are blocks of the Palisades Tuff and Rose Peak Trachyte Members in a landslide deposit at the top of the Husk Windmill Formation. Relatively high stratal accumulation rates in the immediate hanging wall of the Godfrey Peak fault during 30–28 Ma compared to 34–30 Ma (>180 m/Ma compared to 10–20 m/Ma; Fig. 11) are consistent with tectonic activity at that time, but Neogene erosion has removed 30–28 Ma strata from surrounding areas so we cannot compare these accumulation rates with other localities. More work is needed to identify up-section dip changes or wedging that would support 30–28 Ma vertical movement along the Godfrey Peak fault. Movement along the Godfrey Peak fault continued long after 28 Ma because it offsets west-trending felsic dikes in the Godfrey Hills and all west- to northwest-striking faults. This movement also resulted in strata dipping steeply toward the fault and its associated syncline on its immediate hanging wall (generally 20–40°E). This steep east dip and the westward dip near the Alamogordo fault, the latter presumably associated with extensional drape folding or a fault-propagation fold, created the major anticline in the southern Phillips Hills (Fig. 6).

Figures 9 and 12 summarize our tectonic interpretations for the late Eocene and early Oligocene. Because of the lack of preserved late Oligocene and early-middle Miocene strata, we cannot evaluate fault activity during that time period. However, there is no evidence of Quaternary or Pliocene deformation on any of the faults except the Alamogordo fault.

CONCLUSIONS

The present structural configuration of the Sierra Blanca Basin is a composite of different styles and timing of tectonism. The first tectonic event was Laramide contraction. The Eocene Cub Mountain Formation unconformably overlies the Late Cretaceous Crevasse Canyon Formation with a slight angular discordance (Kelley, 1971). Observations that the Cub Mountain-Sanders Canyon stratigraphic interval thickens to the west, that north-south anticlines and synclines are present near the Alamogordo fault, and preliminary subsurface stratigraphic interpretations west of the Alamogordo fault (Koning and Roberts, this volume) indicate Eocene contraction and suggest that the major structures responsible for the Laramide basin were near the Alamogordo fault. There may also have been a component of subsidence from a Laramide releasing bend at the south margin of the basin.

Laramide contraction was followed by post-38 Ma extension and igneous activity. Initial tectonic subsidence occurred during northwest extension that was concomitant with early Sierra Blanca volcanism (38–34 Ma) and emplacement of northeast-striking dike swarms in the eastern and southern margins of the basin. Volcanic flows onlapped pre-38 Ma paleotopography on the south margin of the basin but appear to be conformable with Sanders Canyon Formation strata at the basin's center, which is consistent with 38–34 Ma subsidence centered northwest of Ruidoso. After 30 Ma, there appears to have been a shift of extensional faulting towards the west and the Godfrey Peak fault was active after 28.2 Ma. This shift has continued westward after the Oligocene, since there is no evidence of Quaternary or Pliocene deformation along faults within the Sierra Blanca Basin but indisputable evidence of Quaternary offset along the Alamogordo fault.

ACKNOWLEDGMENTS

We wish to thank Alvis Lisenbee and Steve Cather for their thorough and helpful reviews. Logan Roberts helped draft Figure 10.

REFERENCES

Abbott, J.C., Cather, S.M., and Goodwin, L.B., 1995, Paleogene synorogenic sedimentation in the Galisteo Basin related to the Tijeras-Cañoncito fault system: New Mexico Geological Society, Guidebook 46, p. 271–278.

Allen, M.S. and Foord, E.E., 1991, Geological, geochemical and isotopic characteristics of the Lincoln County porphyry belt, New Mexico: Implications for regional tectonics and mineral deposits: New Mexico Geological Society, Guidebook 42, p. 97–113.

Asquith, B.G., 1974, Petrography and petrogenesis of Tertiary camptonites and diorites, Sacramento Mountains, New Mexico: New Mexico Bureau of Mines and Mineral Resources, Circular 141, 6 p.

Bodine, M.W., Jr., 1956, Geology of Capitan coal field, Lincoln County, New Mexico: New Mexico Bureau of Mines and Mineral Resources, Circular 35, 27 p.

Brown, C.D., and Phillips, R.J., 1999, Flexural rift flank uplift at the Rio Grande rift, New Mexico: Tectonics, v. 18, no. 6, p. 1275–1291.

Cather, S.M., 1990, Stress and volcanism in the northern Mogollon-Datil volcanic field, New Mexico: Effects of the post-Laramide tectonic transition: Geological Society of America Bulletin, v. 102, p. 1447–1458.

Cather, S.M., 1991a, Stratigraphy and provenance of Upper Cretaceous and Paleogene strata of the western Sierra Blanca Basin, New Mexico: New Mexico Geological Society, Guidebook 42, p. 265–275.

Cather, S.M., 1991b, Tectonic overview of the Ruidoso region: New Mexico Geological Society, Guidebook 42, p. 37–39.

Cather, S.M., 1992, Suggested revisions to the Tertiary tectonic history of north-central New Mexico: New Mexico Geological Society, Guidebook 43, p. 109–122.

Cather, S.M., 2002, The Sierra Blanca Basin: New Mexico Geological Society, Guidebook 53, p. 21.

Cather, S.M., Chapin, C.E., and Kelley, S.A., 2012, Diachronous episodes of Cenozoic erosion in southwestern North America and their relationship to surface uplift, paleoclimate, paleodrainage, and paleoaltimetry: Geosphere, v. 8, no. 6, p. 1177–1206.

Cepeda, J.C., 1991, Petrogenesis of the Capitan dike swarm, Lincoln County, New Mexico: Texas Journal of Science, v. 43, p. 111–125.

Chapin, C.E., and Cather, S.M., 1981, Eocene tectonics and sedimentation in the Colorado Plateau-Rocky Mountain area: Arizona Geological Society Digest, v. 14, p. 173–198.

Cikoski, C.T., Koning, D.J., Kelley, S.A., and Zeigler, K.E., 2011 (revised May 2012), Geologic map of the Church Mountain quadrangle, Lincoln County, New Mexico: New Mexico Bureau of Geology and Mineral Resources, Open-file Geologic Map 215, scale 1:24,000.

Cikoski, C., Kelley, S.A., and Koning, D.J., 2012, Geologic map of the Church Mountain 7.5' quadrangle, northern Sacramento Mountains, southeastern New Mexico (abs.): Geological Society of America, Abstracts with Programs - 2012 Rocky Mountain section meeting, v. 44, no. 6, paper no. 8–13.

Dowe, C.E., McMillan, N.J., McLemore, V.T., and Hutt, a., 2002, Eocene magmas of the Sacramento Mountain, NM – subduction or rifting?: New Mexico Geology, v. 24, p. 59–60.

Elston, W.E., and Snider, H.I., 1964, Differentiation and alkali metasomatism in dike swarm complex and related igneous rocks near Capitan, Lincoln County, New Mexico: New Mexico Geological Society, Guidebook 15, p. 140–147.

Goff, F., Kelley, S.A., Lawrence, J.R., Cikoski, C.T., Krier, D.J., Goff, C.J., and McLemore, V.T., 2011, Preliminary geologic map of the Nogal Peak 7.5-minute quadrangle, Lincoln and Otero counties, New Mexico. New Mexico Bureau of Geology and Mineral Resources, Open-file Geologic Map 134, 1:24,000 scale.

Goff, F., Roback, R.C., McIntosh, W., Goff, C.J., and Kluk, E.C., 2014, Geochemistry and geochronology of intrusive and volcanic rocks of the Three Rivers stock, Sierra Blanca, New Mexico: New Mexico Geological Society, Guidebook 65.

Heizler, M., and Dunbar, N.W., 2014, Analytical laboratories at the New Mexico Bureau of Geology: New Mexico Earth Matters, v. 14, no. 1, p. 1–5.

Kelley, V.C., 1971, Geology of the Pecos country, southeastern New Mexico: New Mexico Bureau of Mines and Mineral Resources, Memoir 24, 77 p.

Kelley, V.C., and Thompson, T.B., 1964, Tectonics and general geology of the Ruidoso-Carrizozo region, central New Mexico: New Mexico Geological Society, Guidebook 15, p. 110–121.

Kelley, S., and Kempter, K., 2008, Preliminary geologic map of the Cat Mountain 7.5-minute quadrangle map, Otero County, New Mexico: New Mexico Bureau of Geology and Mineral Resources, Open-file Geologic Map 183, scale 1:24,000

Kelley, S.A., Kempter, K.A., Koning, D.J., Goff, F., Cikowski, C.T., 2011, Preliminary geologic map of the Godfrey Peak 7.5-minute quadrangle, Lincoln and Otero Counties, New Mexico: New Mexico Bureau of Geology and Mineral Resources, Open-file Geologic Map 136, scale 1:24,000.

Kelley, S.A., Koning, D.J., and Allen, B., 2014, Preliminary Geologic Map of the Tularosa and Bent Region, northeastern Tularosa Basin, Otero County, New Mexico: New Mexico Bureau of Geology and Mineral Resources, Open-file Report 563.

Kelley, S.A., Koning, D.J., Goff, F., Cikoski, C., Peters, L., and McIntosh, W., 2014, Stratigraphy of the northwestern Sierra Blanca volcanic field: New Mexico Geological Society Guidebook, 65th Annual Field Conference.

Koning, D.J. and Roberts, L., 2014, Redefinition of the base of the Cub Mountain Formation and preliminary depositional and tectonic interpretations of early-middle Eocene strata in the Sierra Blanca Basin, New Mexico: New Mexico Geological Society, Guidebook 65.

Koning, D.J. and Kempter, K., 2010, Preliminary geologic map of the Carrizozo East 7.5-minute quadrangle, Lincoln County, New Mexico: New Mexico Bureau of Geology and Mineral Resources, Open-file Geologic Map OF-GM-211, scale of 1:24,000.

Koning, D.J., Kelley, S.A., and Goff, F., 2014, Preliminary Geologic Map of the Northeastern Tularosa Basin and Western Sierra Blanca Basin, Lincoln and Otero Counties, New Mexico: New Mexico Bureau of Geology and Mineral Resources, Open-file Report 564.

Lucas, S.G., Cather, S.M., Sealey, P., and Hutchison, J.H., 1989, Stratigraphy, paleontology, and depositional systems of the Eocene Cub Mountain Formation, Lincoln County, New Mexico – a preliminary report: New Mexico Geology, v. 11, p. 11–17.

Mack, G.H., 2004, Middle and late Cenozoic crustal extension, sedimentation, and volcanism in the southern Rio Grande rift, Basin and Range, and southern transition zone of southwestern New Mexico, *in* Mack, G.H., and Giles, K.A., eds., The Geology of New Mexico, A Geologic History: New Mexico Geological Society, Special Publication 11, p. 389–406.

McManus, C.E.D., and McMillan, N.J., 2002, Subduction or rifting: the Eocene magmas of the Sacramento Mountains, NM (abs.): Geological Society of America, Abstracts with Programs, vol. 34, p. 364.

McLemore, V.T., 2002, The Three Rivers Petroglyph Site, Otero County, New Mexico: New Mexico Geological Society, Guidebook 53, p. 26–27.

Miller, W.R., O'Neill, J.M., and McLemore, V.T., 1997, Environmental geochemistry and mineral resource potential of the Three Rivers area and geology of the Three Rivers Petroglyph Site, Otero County, New Mexico: U.S., Department of the Interior, U.S. Geological Survey, Open-file Report 97–444, 36 p.

Moore, S.L., Foord, E.E., Meyer, G.A., and Smith, G.W., 1988. Geologic map of the northwestern part of the Mescalero Apache Indian Reservation, Otero County, New Mexico: U.S. Geological Survey, Miscellaneous Investigations Map I-1895, 1:24,000 scale.

Moore, S.L., Thompson, T.B., and Foord, E.E., 1991, Structure and igneous rocks of the Ruidoso region, New Mexico: New Mexico Geological Society, Guidebook 42, p. 137–145.

New Mexico Bureau of Geology and Mineral Resources, 2003, Geologic Map of New Mexico: New Mexico Bureau of Geology and Mineral Resources, published in cooperation with the U.S. Geological Survey, scale 1:500,000.

Paleobiology Database, 2013, Bridgerian age/stage and Wasatchian age/stage: fossilworks, <http://fossilworks.org/bridge.pl?action=displayInterval&interval_no=231; http://fossilworks.org/bridge.pl?action=displayInterval&interval_no=232> (accessed Nov. 14, 2013).

Peterson, C., and Roy, M., 2005, Gravity and flexure models of the San Luis, Albuquerque, and Tularosa basins in the Rio Grande rift, New Mexico, and southern Colorado: New Mexico Geological Society, Conference 56, p. 105–114.

Pray, L.C., 1961, Geology of the Sacramento Mountains escarpment, Otero County, New Mexico: New Mexico Bureau of Mines and Mineral Resources, Bulletin 35, 144 p.

Rawling, G.C., 2012a, Geology of the Capitan and Nogal Quadrangles, Lincoln County, New Mexico: New Mexico Bureau of Geology, Open-file Report 538, 1:24,000 scale.

Rawling, G.C., 2012b, Geology of the Ruidoso area, Lincoln and Otero Counties, New Mexico: New Mexico Bureau of Geology, Open-file Report 507, 1:24,000 scale.

Rubin, A.M., 1992, Dike-induced faulting and graben subsidence in volcanic rift zones: Journal of Geophysical Research, v. 97, no. B2, p. 1839–1858.

Seager, W., 2004, Laramide (Late Cretaceous-Eocene) tectonics of southwestern New Mexico, *in* Mack, G.H., and Giles, K.A., eds., The Geology of New Mexico, A Geologic History: New Mexico Geological Society, Special Publication 11, p. 183–202.

Thompson, T.B., 1964, A stratigraphic section of the Sierra Blanca Volcanics in the Nogal Peak area, Lincoln County, New Mexico: New Mexico Geological Society, Guidebook 15, p. 76–77.

Thompson, T.B., 1966, Geology of the Sierra Blanca, Lincoln and Otero Counties, New Mexico [Ph.D. dissertation]: Albuquerque, University of New Mexico, 146 p.

Thompson, T.B., 1972, Sierra Blanca igneous complex: Geological Society of America Bulletin, v. 83, p. 2341–2356.

Weber, R.H., 1964, Geology of the Carrizozo quadrangle, New Mexico: New Mexico Geological Society, Guidebook 15, p. 100–109.

Weber, R.H., 1971, K/Ar ages of Tertiary igneous rocks in central and western New Mexico: Isochron/West, No. 71–1, p. 33–45.

Wegemann, C.H., 1914, Geology and coal resources of the Sierra Blanca coal field, Lincoln and Otero Counties, New Mexico: U.S. Geological Survey, Bulletin 541, p. 419–542.